Bioactive Materials 6 (2021) 4786–4800

Contents lists available at ScienceDirect

Bioactive Materials

journal homepage: www.sciencedirect.com/journal/bioactive-materials

Durable endothelium-mimicking coating for surface bioengineering cardiovascular stents

Qing Ma [a,1], Xiuying Shi [a,1], Xing Tan [a], Rui Wang [b], Kaiqin Xiong [a], Manfred F. Maitz [a,c], Yuanyuan Cui [d], Zhangmei Hu [e], Qiufen Tu [a,**], Nan Huang [a], Li Shen [b,***], Zhilu Yang [a,*]

[a] Key Lab of Advanced Technology of Materials of Education Ministry, School of Materials Science and Engineering, Yibin Institute of Southwest Jiaotong University, Southwest Jiaotong University, Chengdu, 610031, China
[b] Shanghai Institute of Cardiovascular Diseases, Department of Cardiology, Zhongshan Hospital, Fudan University, 180 Fenglin Road, Shanghai, 200032, China
[c] Max Bergmann Center of Biomaterials, Leibniz Institute of Polymer Research Dresden, Hohe Strasse 6, 01069, Dresden, Germany
[d] Shimazu China Co. LTD., No. 180 Yizhou Road, Xuhui District, Shanghai, 200233, China
[e] Analysis & Testing Center, Southwest Jiaotong University, Chengdu, 610031, China

ARTICLE INFO

Keywords:
Cardiovascular stents
Nitric oxide
Glycocalyx component
Endothelium mimicking
Surface bioengineering

ABSTRACT

Mimicking the nitric oxide (NO)-release and glycocalyx functions of native vascular endothelium on cardiovascular stent surfaces has been demonstrated to reduce in-stent restenosis (ISR) effectively. However, the practical performance of such an endothelium-mimicking surfaces is strictly limited by the durability of both NO release and bioactivity of the glycocalyx component. Herein, we present a mussel-inspired amine-bearing adhesive coating able to firmly tether the NO-generating species (e.g., Cu-DOTA coordination complex) and glycocalyx-like component (e.g., heparin) to create a durable endothelium-mimicking surface. The stent surface was firstly coated with polydopamine (pDA), followed by a surface chemical cross-link with polyamine (pAM) to form a durable pAMDA coating. Using a stepwise grafting strategy, Cu-DOTA and heparin were covalently grafted on the pAMDA-coated stent based on carbodiimide chemistry. Owing to both the high chemical stability of the pAMDA coating and covalent immobilization manner of the molecules, this proposed strategy could provide 62.4% bioactivity retention ratio of heparin, meanwhile persistently generate NO at physiological level from 5.9 ± 0.3 to $4.8 \pm 0.4 \times 10^{-10}$ mol cm^{-2} min^{-1} in 1 month. As a result, the functionalized vascular stent showed long-term endothelium-mimicking physiological effects on inhibition of thrombosis, inflammation, and intimal hyperplasia, enhanced re-endothelialization, and hence efficiently reduced ISR.

1. Introduction

In 1987, Palmaz and Schatz developed the first balloon-expandable coronary stent made from bare stainless steel. Thanks to the optimization of dual antiplatelet therapy, vascular stent implantation has become one of the most important ways to treat coronary artery diseases, especially for patients with acute coronary syndrome. However, three large-scale clinical trials successively confirmed that implantation of both the bare mental stent (BMS) or drug eluting stent (DES) was not superior to optimal medical therapy in the treatment of patients with stable coronary heart disease [1–3], which raised questions about the necessity and effectiveness of coronary stent implantation. The reason may be that the increasingly serious complications after stent implantation, such as in-stent restenosis (ISR) [1] and late stent thrombosis (LST) [3], annihilate the improved coronary flow reserve. Based on the comprehensive analysis of the mechanism, it is found that endothelial dysfunction plays a key role in inducing these complications. The occurrence of LST and very late stent thrombus (VLST) after implantation of the first-generation DES (G1-DES) was mainly attributed to the absence or delayed endothelialization, which was caused by the loaded

Peer review under responsibility of KeAi Communications Co., Ltd.
* Corresponding author.
** Corresponding author.
*** Corresponding author.
E-mail addresses: tuqiufen@swjtu.edu.cn (Q. Tu), shen.li1@zs-hospital.sh.cn (L. Shen), zhiluyang1029@swjtu.edu.cn (Z. Yang).
[1] Q. Ma and X. Shi contributed equally to this work.

https://doi.org/10.1016/j.bioactmat.2021.05.009
Received 4 May 2021; Received in revised form 10 May 2021; Accepted 10 May 2021
Available online 24 May 2021

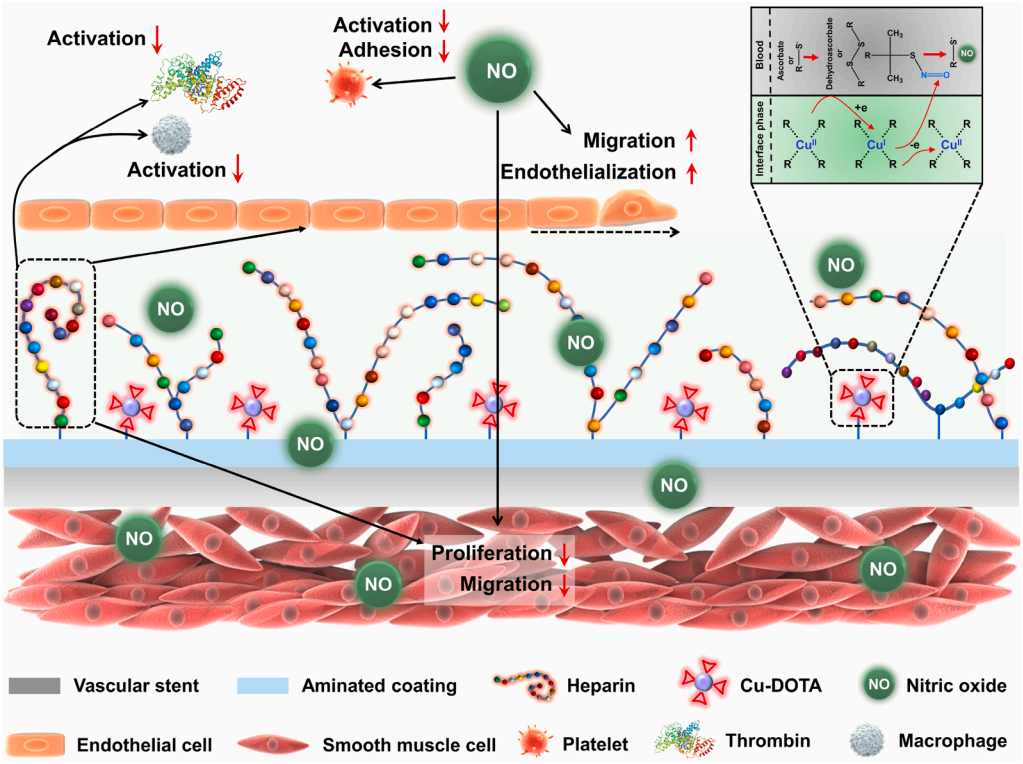

Fig. 1. The durable endothelium-mimicking coating for surface bioengineering of cardiovascular stents is achieved by covalent immobilization of NO producing substance Cu-DOTA coordination complex and bioactive molecule heparin. The coating combines the functions of NO and heparin for improved inhibition of thrombogenic responses (coagulation cascade and platelets) and inhibition of SMC proliferation, thereby reducing the risk of thrombosis and stenosis of the stent.

drug, such as rapamycin and paclitaxel [4]. Endothelialization of the second-generation DES (G2-DES) has been significantly improved by replacement with everolimus or zotarolimus, which have less toxicity to endothelial cells (ECs) than rapamycin and paclitaxel. However, Otsuka et al. demonstrated that there was no significant difference in the occurrence of neo-atherosclerosis (neo-AS) between G1- and G2-DES [5]. Endothelial dysplasia was assumed to be responsible for the accelerated neo-AS in DES-ISR, including the poor cell-to-cell junctions, the reduced expression of anti-thrombotic molecules, and the decreased nitric oxide (NO) production [6,7]. Therefore, building an endothelium-mimicking interface on a vascular stent to endow the stent with natural endothelial functions, may be an effective way to reduce the complications of stent implantation.

Tethering bioactive molecules secreted by ECs on the stent surface is frequently performed to mimic endothelium function. The most popularly selected molecules include the heparin and NO-releasing systems [8,9]. Heparin, one of the major glycoproteins in endothelial glycocalyx, is originally recognized as an anticoagulant [10], which has also proven to be able to inhibit migration [11] and proliferation [12] of smooth muscle cells (SMCs), and to reduce inflammation [13]. However, heparin-modified stents sometimes failed to inhibit intimal hyperplasia, and may even promote it [14–16]. One possible speculation was that the single molecule is not sufficient to deal with the complicated physiological and pathological processes after stent implantation [17]. Meyerhoff et al. pointed out that there is no single natural molecule which can block both the intrinsic and extrinsic coagulation pathways, so they synthesized a heparin derivative with NO releasing property for a better anticoagulant performance [18]. NO has been uncovered to have multiple physiological functions, including anti-coagulation [19–21], anti-inflammation [22] and inhibition of SMCs [23,24]. It is worth pointing out that NO exhibits the antithrombotic and anti-proliferative functions via different pathways from heparin. The anticoagulant activity of heparin is achieved mainly by catalyzing the combination of antithrombin III (AT III) and thrombin [25–27], while NO acts by inhibiting platelet activation and aggregation [28]; heparin inhibits SMCs migration and proliferation mainly via extracellular signal-regulated kinase (ERK) and/or protein kinase C (PKC) signaling pathway [29], while NO acts via the cyclic guanosine monophosphate (cGMP) pathway [30].

The synergistic system of NO and heparin that Meyerhoff et al. constructed via synthesis of a heparin derivative with NO releasing properties, had the common problem of NO releasing system, that is, a burst in the early stage and rapid exhaustion [31]. In our previous study, we have developed several systems based on NO catalytic release and biomolecule co-immobilization, in which NO release was more stable and lasted for a longer time. Firstly, heparin and the NO-generating molecule selenocystamine (SeCA) were co-immobilized on a plasma polymerized allylamine coating (PPAam) on a vascular stent for improved endothelialization and inhibition of ISR [32]. Then, SeCA was replaced with Cu-DOTA (1,4,7,10-Tetraazacyclododecane-N,N′,N″,N‴-tetraacetic acid) coordination complex to obtain a higher NO catalytic bioactivity [33]. Moreover, we also constructed a widely applicable metal-catechol-amine coating, in which Cu^{2+} were coordinated with different numbers of phenolic hydroxyl groups (2, 4, or 6) to generate NO, and amino groups for grafting of heparin [8]. However, the coordination ability of Cu^{2+} with catechols was not strong enough, so the Cu^{2+} was inevitable to escape from the coating in the process of NO catalysis. After soaking in NO donor solution for 15 d, only 50% of the initial NO release rate was remained.

To meet long-term functional requirements of cardiovascular stents, a durable endothelium-mimicking surface is therefore necessary. Herein, we designed a robust mussel-inspired amine-bearing adhesive coating (pAMDA) for tailoring endothelium-mimicking functionalities (Fig. 1, Fig. 2A). The pAMDA coating was formed by pretreatment with pDA, followed by surface chemical cross-link with pAM. The pAMDA coating had a universal and strong adhesive property, basic

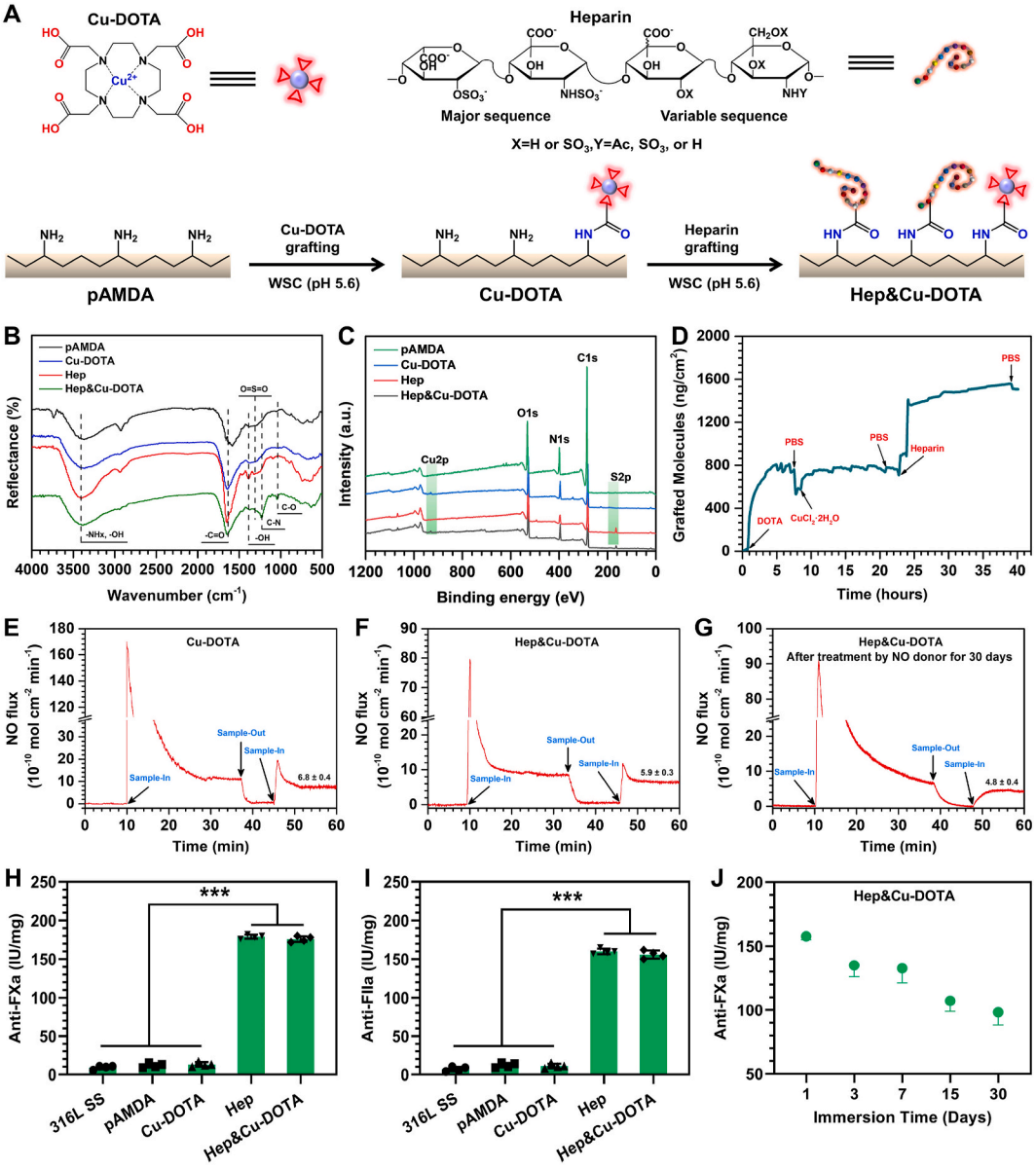

Fig. 2. (A) Cu-DOTA and heparin were stepwisely covalently immobilized on the amine-bearing pAMDA coating based on carbondiimine chemistry. (B) GATR-FTIR spectra and (C) XPS wide-scan survey spectra of the coatings. (D) Real-time monitor of molecule grafting by QCM-D. Real-time release of NO induced by Cu-DOTA (E) and Hep&Cu-DOTA before (F) and after (G) treatment with PBS (pH 7.4) containing NO donor for 30 d. (H, I) Anti-factor Xa and IIa activity of the Hep and Hep&Cu-DOTA coatings and (J) anti-factor Xa activity after treatment with PBS (pH 7.4) for different time intervals. Data are presented as mean ± SD (n = 4) and analyzed using a one-way ANOVA. A p-value less than 0.05 is statistically significant. The symbol *** indicates $p < 0.005$.

characteristics of catechol-amine coatings, and also contained a large number of amino groups, introduced by pAM, for covalent grafting of stable Cu-DOTA coordination complex to catalyze the NO release at a physiological rate (referred to as Cu-DOTA), or/and enough amount of heparin to effectively inhibit blood coagulation and SMCs proliferation (referred to as Hep and Hep&Cu-DOTA, respectively). The high chemical stability of both the pAMDA coating and Cu-DOTA complex imparted the endothelium-mimicking stents with about 62.4% of heparin bioactivity retention and up to 81.3% of catalytic activity of NO after application for 1 month.

2. Materials and methods

2.1. Materials

316L stainless steel (SS) substrates were processed by Chengdu Derbo Steel Co., Ltd; dopamine hydrochloride, pAM solution, DOTA, and copper (II) chloride hydrate ($CuCl_2{\cdot}2H_2O$, 99%) were purchased from Aladdin Reagents Co., Ltd.; ethanol, isoamyl acetate, hydrochloric acid, acetone, sodium chloride and sodium hydroxide were purchased from Chengdu Kelong Chemical Reagents Co., Ltd.; quartz sensor crystals were purchased from Jiaxing Jingkong Electronic Co., Ltd.; N-(3-Dimethylaminopropyl)-N′-ethylcarbodiimide hydrochloride (EDC), N-hydroxysuccinimide (NHS) and 2-(N-morpholino) ethanesulfonic acid hydrate (MES) were purchased from Sigma-Aldrich Corp.; NHS-Fluorescein isothiocyanate (NHS-FITC, 90%) was bought from Thermo Fisher Technology Co., Ltd.; phosphate buffered saline solution (PBS), Tris-buffered saline solution (TBS) and trypsin were purchased from Hyclone Laboratories; Cell culture medium for ECs and SMCs were purchased from Vasculife® by Lifeline Cell Technology Co., Ltd.; Chromogenix Coamatic® Heparin test, used to measure the anticoagulant activity of heparin, was purchased from Chromogenix Co., Ltd.;

activated partial thromboplastin time (APTT) reagent was purchased from Shanghai Sun Biotech Co., Ltd.; mouse anti-human fibrinogen/HRP, goat anti-mouse IgG/HRP, and anti-fibrinogen gamma chain antibody were purchased from Beijing Biosynthesis Biotechnology Co., Ltd.

2.2. Preparation of the amine-bearing coating

To obtain an aminated surface for supporting co-immobilization of the Cu-DOTA coordination complex and heparin, the 316L SS substrate was firstly pre-coated with pDA via the self-polymerization of dopamine by a one-step dipping method [34]. In brief, the mirror polished 316L SS substrates were immersed into dopamine solution in TBS (0.01 M, pH 8.5), and then incubated at 37 °C under aerobic conditions. After incubation for 24 h, the pDA-coated substrates were ultrasonically cleaned in ultrapure water to eliminate physically adsorbed species and dried with nitrogen gas. Subsequently, pDA-coated substrate was further treated by pAM solution for a robust aminated coating through the catecholic-amine chemical crosslinking, and the coating is referred to as pAMDA.

2.3. Co-immobilization of the Cu-DOTA coordination complex and heparin

The Cu-DOTA coordination complex and heparin were sequentially grafted on the pAMDA-modified substrates using carbodiimide chemistry. Briefly, DOTA (10 μg/mL) was firstly pre-dissolved in water-soluble carbodiimide solution system (WSC, pH 5.6), with EDC (1 mg/mL) and NHS (0.24 mg/mL) dissolved in MES buffer solution (pH 5.6), for 30 min. Then, $CuCl_2{\cdot}2H_2O$ with 1:1 of molar ratio to DOTA was added to form Cu-DOTA coordination complex. After that, the pAMDA-coated substrates were immersed into the above solution for 12 h to immobilize the Cu-DOTA complex. The subsequent grafting of heparin is similar to that of the Cu-DOTA complex. The Cu-DOTA-modified substrates were immersed into heparin sodium salt solution (1 mg/mL) dissolved in WSC solution for 12 h to realize the tethering of heparin, which was marked as Hep&Cu-DOTA. Substrate functionalized only by Cu-DOTA coordination complex or heparin was denoted as Cu-DOTA and Hep, respectively.

2.4. Characterization of the functional coatings

The chemical structures of the coatings were examined by grazing angle attenuated total reflection Fourier transform infrared spectroscopy (GATR-FTIR, NICOLET 5700).

X-ray photoelectron spectroscopy (XPS, AXIS Supra, Kratos Analytical Inc., JP) was employed to identify the chemical components of the coatings. The selection of X-ray source and the setting of test parameters refer to the study of Zhang et al. [35].

An ultraviolet spectrophotometer (TU-1901, Beijing Puxi General Instrument Co, Ltd., China) was used to determine the coordination of copper ions with DOTA.

The thickness of the coatings was measured using a spectroscopic ellipsometer (W-VASE, J.A.Woollam, USA), and their ψ (±0.015°) and Δ (±0.08°) values were calculated in a wavelength range from 240 to 1100 nm.

Scanning electron microscopy (SEM, JSM-7800F, JEOL Ltd., JP) was used to analyze the morphology of the coatings on vascular stents before and after stent dilation by an angioplasty balloon, with a stent diameter change from 1.65 to 2.75 mm. SEM detection was operated at 2.7 kV × 15 mA under a pressure of 5×10^{-4} Pa.

An acid Orange II (AO II) assay was used to quantify the total amount of amino groups (including the primary, secondary, and tertiary amino) of the coatings. Briefly, the samples were immersed into 500 μL of AO II solution (1.75 mg/mL, pH 4.0), and then incubated for 8 h at 37 °C. Then the samples were taken out and washed with HCl solution (pH 4.0) for 3 times and dried. Subsequently, the dried samples were incubated with 170 μL of NaOH solution (0.4 mg/mL) for 30 min at room temperature to elute the adsorbed AO II. Finally, the eluted solution was transferred to a 96-well plate and measured by a microplate spectrophotometer (Epoch, Biotek, USA) at 485 nm. At the same time, AO II solutions with a series of gradient concentrations were prepared and measured for a standard curve.

Water contact angles (WCA) were determined by a Krüss GmbH DSA 100 Mk 2 goniometer (Hamburg, Germany) for evaluating the wettability of the coatings.

2.5. Catalytic release rate of NO

With the help of a NO analyzer (NOA, Seivers 280i, Boulder, CO), a chemiluminescence method was adopted to real-time monitor the release of NO. 316L SS foils (0.5 cm × 1 mm) coated with Cu-DOTA and Hep&Cu-DOTA were used to probe the NO release rate. NO donor solution was prepared by dissolving L-glutathione (GSH, an endogenous reductant, 10 μM) and NO donor S-nitroso-N-acetyl-DL-penicillamine (GSNO, a nitrosothiol derivative, 10 μM) in PBS (pH 7.4). After 8 min of baseline equilibration, the Cu-DOTA- or Hep&Cu-DOTA-coated 316L SS foil was dipped in the NO donor solution, and the release of NO was recorded in real-time each quarter of a second. After reaction for about 40 min, the samples were removed from the NO donor solution. When the base line remained stable for about 10 min, the sample was immersed into the reaction solution again to study its catalytic stability. All the processes were carried out at 37 °C in the absence of light.

2.6. Quartz crystal microbalance with dissipation (QCM-D) measurement

QCM-D (Bioolin Technology Co, Ltd, Sweden) was used to quantitatively test the amount of DOTA-Cu and heparin molecules grafted on the pAMDA surface in real-time. Firstly, the quartz wafer (Ø 1 cm, 5 MHz) was precoated with pAMDA coating and installed correctly in the QCM-D chamber. Then, MES buffer solution (pH 5.6) was pumped into the chamber at a flow rate of 50 μL/min, and the frequency change of the quartz crystals was recorded. After a plateau was reached, 10 μg/mL of DOTA activated by WSC solution was pumped into the chamber until the frequency was stable, then PBS solution (pH 7.4) was pumped to remove the physically adsorbed DOTA. Subsequently, $CuCl_2{\cdot}2H_2O$ with 1:1 of molar ratio to DOTA dissolved by PBS (pH 7.4) and 1 mg/mL of heparin sodium salt activated by WSC were respectively pumped into the chamber for realizing their tethering onto the pAMDA-coated surface. Finally, the Sauerbrey equation was adopted to convert the frequency change into mass change using the Q-Tools software [36].

2.7. Anti-Factor Xa and IIa activity by heparin

Anti-Factor Xa and IIa activities of the immobilized heparin in the Hep and Hep&Cu-DOTA-functionalized surfaces were evaluated by using Chromogenix Factor Xa and Factor IIa Kits (COAMATIC® heparin, Milano, Italy), respectively. Firstly, 10 μL of platelet-poor plasma (PPP) diluted by 40 μL of PBS was spread onto the sample surface and incubated at 37 °C for 30 min to form the heparin-AT III complex. Then, 50 μL of chromogenic substrate S-2732 plus 50 μL of Factor Xa, or S-2238 plus Factor IIa was supplemented, respectively, and incubated at 37 °C for 2 min. After that, 100 μL of the above incubated solution from each sample was collected in a 96-well plate, and 50 μL of citric acid (2%) was then added to stop the reaction. The absorbance at 405 nm was detected by a microplate spectrophotometer. The absorbance value was inversely proportional to the heparin activity on the samples. To evaluate the long-term activity of the grafted heparin, the samples were incubated in 5 mL PBS (pH 7.4) and shaked on an oscillator at 37 °C for 1, 3, 7, 15, and 30 d. The PBS solution was replaced every 12 h. Then, the anti-Factor Xa and IIa activities of the heparin bound to the samples treated by PBS were determined.

2.8. Cell culture

All cells were subcultured in a cell culture incubator, with 5% CO_2 at 37 °C. Human umbilical vein endothelial cells (HUVECs), human umbilical artery smooth muscle cells (HUASMCs) and Raw 264.7 macrophages were purchased from Shanghai Zhong Qiao Xin Zhou Biotechnology Co., Ltd. HUVECs and HUASMCs were cultured in ECs culture medium (ECM) and SMCs culture medium (SMCM, PromoCell GmbH, Heidelberg, Germany). Macrophages were incubated in Dulbecco's Modified Eagle Medium (DMEM, high glucose type, Bioind, Beit-Haemek, Israel) supplemented with L-glutamine, 10% fetal bovine serum (FBS) and 1% Penicillin-Streptomycin (PS, Sigma-Aldrich, USA). When the cells reached about 80% confluence, subculture was carried out, and cells from passage 3 to 8 were used in this study.

2.9. Cell adhesion and proliferation

The cells (HUVECs, HUVSMCs or macrophages) were seeded on the samples in 24-well cell culture plates at a density of 2.0×10^4 cells/mL, respectively, and incubated in their corresponding culture medium supplemented with NO donors (10 μM GSNO and 10 μM GSH). After incubating for 2, 24, and 72 h, the samples were rinsed with PBS, and fixed with 4% paraformaldehyde (Bioind). After that, the cells grown on the sample surfaces were stained with Rhodamine 123 and observed by a fluorescence microscope (CKX53, OLYMPUS, Japan). For 24 and 72 h of incubation, the cell viability was detected by Cell Counting Kit-8 (CCK-8 Kit) according to the manufacturer's instruction.

2.10. Cell migration

316L SS foil slices (1 cm × 2 cm) were used for cell migration assays. Each slice was folded in half from the middle of the long axis to form a vertical angle; one of the folded sides had the functional coating, while the other was uncoated. The samples were placed in a 24-well cell culture plate with the non-modified side at the bottom of the well, and then cells were seeded at a density of 5×10^5 cells/mL. After 6 h of culture, a confluent cell layer was formed, the culture medium was removed, and the samples were rinsed with PBS to remove the non-adherent cells. Then, the samples were turned over to place the modified side at the bottom of the well, and fresh cell culture medium supplemented with NO donor was added to facilitate the cells migration from the non-modified side to the modified side. After 24 h, all the samples were collected, washed with PBS, fixed with 4% paraformaldehyde, stained with rhodamine 123, and finally observed with a fluorescence microscope.

2.11. Co-culture of HUVECs and HUVSMCs

HUVECs and HUVSMCs were pre-labeled with green chloromethyl fluorescein diacetate (CMFDA) and orange chloromethyl trimethyl rhodamine (CMTMR), respectively, following the manufacturer's instruction. Then, the pre-labeled HUVECs and HUVSMCs were trypsinized to prepare cell suspensions with the same density (5×10^4 cells/mL); 0.5 mL of HUVECs and 0.5 mL of HUVSMCs cell suspension were subsequently mixed and added to each sample in a 24-well plate. After 2 and 24 h of incubation, the samples were observed and photographed with a fluorescence microscope for counting the ratio of both kinds of cells. No less than 12 micrographs of each sample were taken for statistical analysis.

2.12. Expression of pro-inflammatory and anti-inflammatory factors in macrophages

When the macrophages were cultured on the bare and coated 316L SS samples for 24 h, the supernatant was collected and centrifuged at 3000 rpm for 5 min to remove the cells and debris. Then, the pro-inflammatory (IL-1β, IL-6, and TNF-α) and anti-inflammatory factors (IL-10, TGF-β, and IL-23) in the supernatant were simultaneously detected by using BioLegend's LEGENDplex™ bead-based immunoassays. The experiments were performed according to the manual. The immunofluorescence (IF) signals of 5000 LEGENDplex™ beads were recorded for each sample, and the number of positive beads of different inflammatory factors was counted and transferred into percentage of positive beads, thus indirectly reflecting the expression of this factor.

2.13. Blood collection

Fresh human whole blood was collected from healthy volunteers, who were requested to fast from midnight before drawing blood. All blood samples were anticoagulated with trisodium citrate (3.5% wt) at an anticoagulant/blood ratio of 1:9. Platelet-rich plasma (PRP) was prepared by centrifugation of the whole blood at 1500 rpm for 15 min, for subsequent platelet adhesion experiments. Platelet-poor plasma (PPP) was obtained by centrifuging whole blood at 3000 rpm for 15 min, for subsequent fibrinogen (Fg) adsorption and activation experiments. The experiments were performed in compliance with ethical norms and relevant laws.

2.14. Platelet adhesion and activation

PRP was pre-incubated at 37 °C for 10 min. Then, 200 μL of PRP supplemented with NO donor was added on each sample in a 24-well plate, and incubated at 37 °C for 30 min. After that, the samples were rinsed 3 times with PBS to remove non-adherent platelets. Part of the samples were fixed with 2.5 wt% glutaraldehyde solution for 12 h for SEM inspection. In brief, the samples were thoroughly washed, dehydrated with gradient concentrations of ethanol, and dealcoholized with increasing concentrations of isoamyl acetate. After drying in vacuum, the samples were sputtered with gold and examined by SEM. For cGMP expresssion test of the platelets, the platelets adhered on the samples were ultrasonically crushed with each 100 μL of Triton X-100 solution (10%), and then the platelet lysate was centrifuged at 2500 rpm for 15 min. Finally, the obtained supernatant was collected for cGMP detection using a cGMP ELISA kit, refering to the Kit instruction.

2.15. Fibrinogen adsorption and activation

For the test of adsorption of fibrinogen (Fg), 100 μL of PPP was spread on each sample surface. After incubation at 37 °C for 2 h, the samples were washed 3 times with PBS and blocked with 250 μL of 5% BSA (bovine serum albumin) solution for 30 min. Then, 50 μL of mouse anti-human Fg/HRP antibody (1:1000) was dropped on each sample and incubated at 37 °C for 1 h. Afterward, 100 μL of chromogenic substrate 3,3′,5,5′-Tetramethylbenzidine (TMB, composed of A and B solutions with the ratio of 1:1) was added to each sample. After reaction for 10 min, 50 μL of H_2SO_4 solution (1 M) was added to quench the reaction. The absorbance was read at 450 nm by a microplate spectrophotometer.

Activation of Fg adsorbed on the sample surface was indirectly evaluated by determing the amount of Fg gamma chain. Fg was pre-adsorbed on the sample for 2 h and then blocked with BSA as described above. Subsequently, 50 μL of anti-fibrinogen gamma chain antibody (1:3000) was added on each sample surface and incubated at 37 °C for 1 h. Next, the sample was incubated with 50 μL of the goat anti-mouse IgG/HRP at 37 °C for 1 h. After that, the subsequent chromogenic steps and absorbance detection were the same as those of Fg adsorption.

2.16. Hemolysis test

A hemolysis test is required for the evaluation of a foreign blood-contacting material. In detail, 10 mL of whole blood was first collected and mixed with 8 mL of 0.9% saline solution. Then, the sample was incubated with 10 mL of saline solution at 37 °C for 30 min. After

that, 0.2 mL of diluted whole blood was added and incubated at 37 °C for 1 h. Saline solution of equal volume was selected as a negative control while deionized water was regarded as a positive control in this test for calculation of hemolysis degree. The incubated solution was collected and centrifuged at 3000 rpm for 5 min, and the absorbance of the released hemoglobin from red blood cells was detected using a microplate reader at 540 nm. The hemolysis degree was calculated according to the following formula:

$$\%\ Hemolysis = [(Aa - Ac)/(Ab - Ac)] \times 100 \quad (1)$$

where Aa refers to the absorbance value of samples, Ab and Ac are the absorbance values of the positive group and negative group, respectively.

2.17. Ex-vivo and in vivo evaluation of anti-thrombogenicity

To better simulate the real flowing condition of blood, *ex-vivo* circulation experiments using New Zealand white rabbits were carried out in this study, as described in detail elsewhere [8,33]. All the animal experiments comply with the Chinese National Guidelines for the Care and Use of Laboratory Animals. Six rabbits (2.5–3.5 kg) and four parallel samples of each group were used in this test. The uncoated-, and pAMDA-, Cu-DOTA-, Hep- and Hep&Cu-DOTA-coated 316L SS foils (8 mm × 12 mm) were coiled and installed in the inner wall of an arterial-venous extracorporeal circuit (ECC). The ECC was constructed by connecting the left carotid artery and the right jugular vein with a commercial surgical catheter. All the rabbits were pre-injected with NO donor at a dose of 1 mL/kg. The blood flow in the catheter was monitored for as long as 2 h. Then, the catheters installed with samples were collected and photographed. The foils were taken out, weighed, photographed, washed and fixed with 2.5% glutaraldehyde solution for 12 h for SEM inspection.

Two hours of *in vivo* stent implantation was further performed to evaluate the thromboprotective effect of the Hep&Cu-DOTA coatings. First of all, uncoated- and Hep&Cu-DOTA-coated 316L SS vascular stents (Ø 2.75 mm, length 1.65 mm, n = 4) were installed onto balloons. Four New Zealand white rabbits (2.5–3.5 kg) were anesthetized and used for the *in vivo* stent implantation. The uncoated- and Hep&Cu-DOTA-coated 316L SS vascular stents were implanted in the opposite sides of the iliac arteries, respectively. After 2 h of implantation, the arteries with implanted stents were collected, washed, fixed with 2.5% glutaraldehyde, and finally cut along the long axis for SEM analysis.

2.18. In vivo stent implantation for the evaluations of re-endothelialization and restenosis

Eight New Zealand white rabbits were used for the evaluations of re-endothelialization and restenosis. All the rabbits were randomly and evenly divided into two groups, for 1 month and 3 months implantation. After stent implantation, the rabbits were intravenously injected with benzylpenicillin (0.3 mega IU/kg/day) for 5 d. The iliac arteries containing the vasular stents were collected for re-endothelialization and restenosis evaluation after 1 and 3 months implantation.

In detail, the harvested samples were thoroughly washed with heparinized saline and saline solution, and then cut transversely into two halves from the middle of the stent. One half was fixed with 10% formaldehyde for resin embedding to study intimal hyperplasia. The other half was further cut longitudinally into two halves, one of which was fixed with 2.5% glutaraldehyde for SEM evaluation of re-endothelialization, and the other half was fixed with 4% paraformaldehyde for CD31 immunofluorescence staining to further identify the cells grown on the stents. For the CD31 staining, the fixed artery tissue containing stent was washed with PBS, treated with Triton X-100 solution (0.5% in PBS) for 10 min, blocked with BSA solution (1% in PBS) for 30 min, and incubated with 2 μg/mL mouse anti-rabbit CD31/PECAM-1 antibody overnight at 4 °C. After that, the stent containing tissue was carefully washed and stained with the Absin™ 488-conjugated anti-mouse IgG secondary antibody (abs200013, 2 μg/mL) for 2 h and counterstained with 4',6-diamidino-2-phenylindole dihydrochloride (DAPI) for 10 min. The tissue was finally stained with phalloidin YF555 (5 μg/mL, Everbright Inc., US) at 37 °C for 1 h, thoroughly washed, and observed with a laser confocal microscope (LSCM, A1R$^+$, Nikon, Japan), and a software of NIS Viewer (v.4.5, Nikon Instruments Inc. Japan) was employed to analyze and process the data.

The vascular tissue with the stent for restenosis evaluation were first washed with heparinized saline and saline solution. Then, they were dehydrated with gradient concentrations of ethanol, and dealcoholized with xylene. After that, they were infiltrated in a mixed solution of methyl methacrylate and dibutyl phthalate, and finally solidificated in this polymer solution supplemented with benzoyl peroxide as initiator. The obtained resin embedding tissues were subsequently cut into thin slices with a thickness of about 100 μm by using a hard tissue slicer (Xi'an Lanming Medical Technology Co., Ltd, China) and stained with Van Gieson stain. Histological micrographs were taken to measure and analyze neointimal thickness, and the results are presented as mean ± standard deviation (SD, n = 4).

2.19. Statistical analysis

All the experimental data are presented as mean ± SD (n = 4). Significant levels among groups were compared using a one-way analysis of variance (ANOVA) by IBM statistical software (v.20, SPSS, Chicago, IL, USA). *In vitro* studies were performed in three independent experiments with at least four technical replicates. A p-value of ≤ 0.05 was considered to be statistically significant between groups.

3. Results and discussion

3.1. Characterization of the endothelium-mimicking coating

The endothelium-mimicking coating was fabricated via a two-step procedure: 1) construct a durable pAMDA adhesive coating rich in amino groups on the 316L SS surfaces (Fig. S1); 2) stepwise synergistic grafting of NO-generating species (Cu-DOTA coordination complex) and glycocalyx-like component (heparin) by using carbodiimide chemistry (Fig. 2A). The pDA-like dark-brown color of the modified vascular stent confirmed the successful deposition of the pAMDA coating (Fig. S1B, left). To test the reactivity of surface amino groups, NHS-FITC was used to functionalize the pAMDA coating. The visible green fluorescence on the stent profile detected at 491 nm demonstrated the secondary reaction of surface amino groups for grafting molecule (Fig. S1B, right). Next, Cu-DOTA coordination complex (Fig. S2A) and heparin were used for tailoring surface endothelium-mimicking functionalities. After grafting Cu-DOTA or/and heparin to pAMDA, the peak between 3100 and 3600 cm^{-1} in the GATR-FTIR spectra was significantly broadened, which may be due to the introduction of -OH stretching vibration peaks by both molecules with a large amount of carboxyl groups. Moreover, the band intensity of C═O stretching vibration (1640 cm^{-1}) and C-N deformation vibration (1220 cm^{-1}) was remarkably reinforced, indicating the successful amidation reaction between -COOH of Cu-DOTA or heparin and -NH_2 of pAMDA coating (Fig. 2B). Additionally, the emergence of two characteristic peaks of heparin, namely bending vibration of -OH (1400 cm^{-1}) and stretching vibration of O═S═O (1320 cm^{-1}) in the Hep and Hep&Cu-DOTA coatings also confirmed the successful immobilization of heparin in the pAMDA coating. To further confirm the successful immobilization of Cu-DOTA and heparin, surface characterization of the pAMDA coating before and after grafting of Cu-DOTA or/and heparin was carried out by XPS. Clearly, the copper and sulfur specific to the Cu-DOTA and heparin were respectively detected at 933.6 eV in both the Cu-DOTA and Hep&Cu-DOTA coatings, and 168.3 eV in both the Hep and Hep&Cu-DOTA coatings (Fig. 2C), which verified

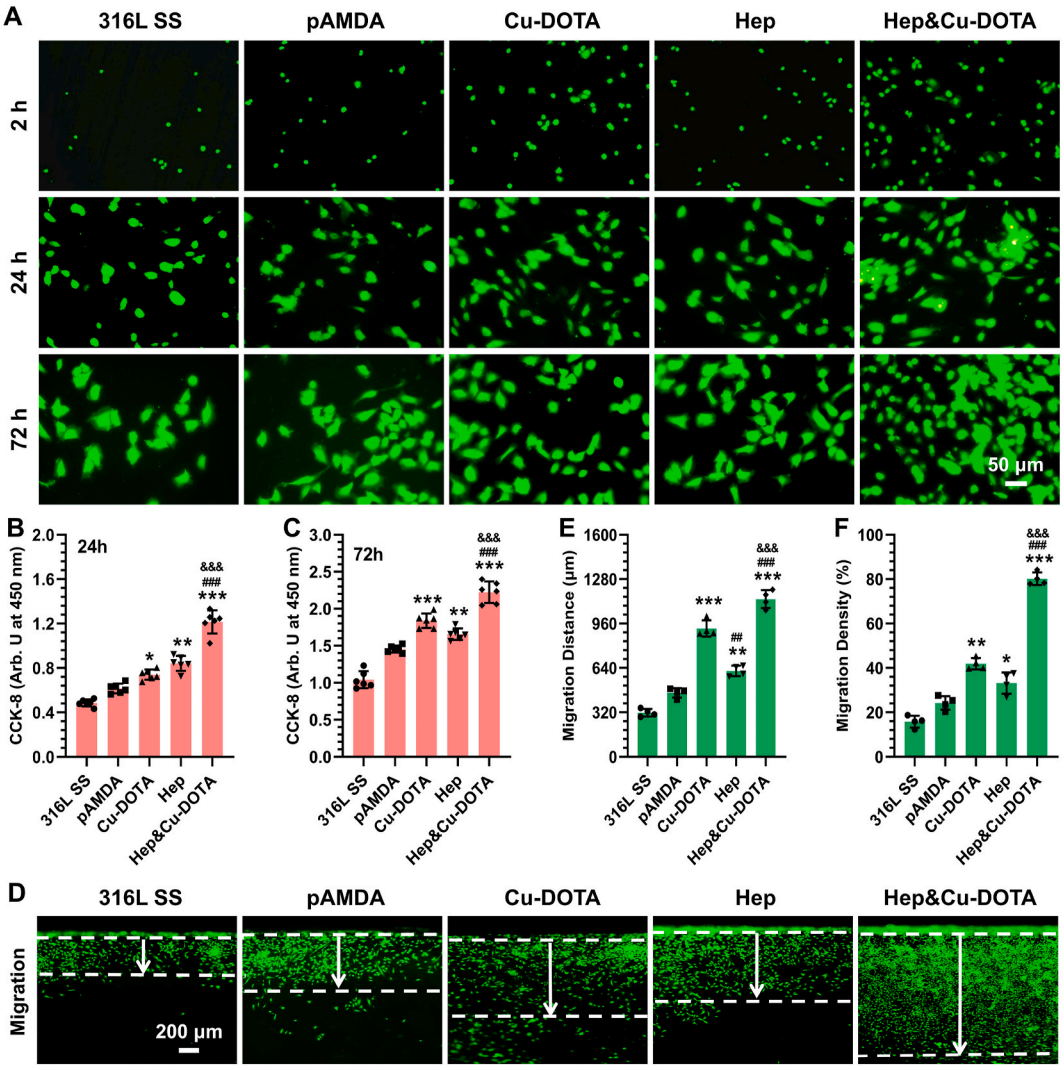

Fig. 3. Adhesion, proliferation and migration of HUVECs on the non-modified and pAMDA-, Cu-DOTA-, Hep-, and Hep&Cu-DOTA-modified 316L SS. (A) Fluorescence micrographs of HUVECs grown on these surfaces; cell viability after 24 (B) and 72 h (C) of incubation was determined using a CCK-8 kit; (D) Fluorescence micrographs of HUVECs migrated on the above surfaces for 24 h; migration distance (E) and migration density (F) calculated from the fluorescence micrographs. Data are presented as mean ± SD (n = 4) and analyzed using a one-way ANOVA (* compared with pAMDA, # with Cu-DOTA and & with Hep; one symbol indicates $p < 0.05$, two symbols indicate $p < 0.01$ and three symbols indicate $p < 0.005$).

the effective immobilization of Cu-DOTA or/and heparin on the pAMDA coating. Moreover, the obvious changes in the densities of surface amino groups (Fig. S1C) and the contents of oxygen (Table S1) of the Cu-DOTA, Hep and Hep&Cu-DOTA also confirmed the immobilization of Cu-DOTA and heparin on the pAMDA coating. Real-time monitor of the molecules bound to the pAMDA-coated surface by QCM-D revealed that the DOTA molecule was effectively tethered on the pAMDA coating at ~623 ng/cm^2 after 8 h, and then approximately 162 ng/cm^2 of Cu^{2+} ions was chelated to the DOTA (Fig. 2D). The residual primary amino groups on the pAMDA supported the further conjugation of about 801 ng/cm^2 of heparin. The significant changes in surface wettability also further confirmed the effective grafting of Cu-DOTA and heparin on pAMDA coating (Fig. S3 A, B). As a coating used for surface engineering of a vascular stent, it showed excellent adhesion strength and flexibility to follow the deformation of the stent (Fig. S4), implying the potential application of such an endothelium-mimicking coating in vascular stents.

To examine the *in vitro* NO catalytic behavior of both Cu-DOTA- and Hep&Cu-DOTA-coated 316L SS substrates, a chemiluminescence assay was carried out. Firstly, real-time monitoring of NO release of 316L SS substrates grafted with Cu-DOTA coordination complex prepared by 10 μg/mL of DOTA and $CuCl_2{\cdot}2H_2O$ with different feed concentrations from 0.01 to 5 μg/mL to optimize the release rate of NO that is suitable for vascular stents. (Fig. S2). In our previous work, we demonstrated that the NO release rate ranging from 6 to 8 × 10^{-10} mol cm^{-2} min^{-1} was suitable for tailoring an ideal vascular stents with multiple physiological functions [24]. Finally, an ideal NO release rate of 6.8 ± 0.4 × 10^{-10} mol cm^{-2} min^{-1} was optimized by feeding 5 μg/mL $CuCl_2{\cdot}2H_2O$ for preparing the Cu-DOTA-functionalized surface (Fig. S2 B). The further immobilization of heparin led to a slight decrease in NO release rate from 6.8 ± 0.4 to 5.9 ± 0.3 × 10^{-10} mol cm^{-2} min^{-1}. The decreased NO catalytic generation might be ascribed to the loss of unstably chelated Cu^{2+} to the DOTA bound to the pAMDA coating or shielding effect induced by immobilized heparin (Fig. 2E and F). It was noteworthy to mention that the continuous treatment of the Hep&Cu-DOTA substrate with NO donor solution for 30 d only resulted in a loss of 18.7% of NO release rate (Fig. 2G), which is significant lower than the previously reported values [8,32,33], implying the durable NO catalytic activity and potential long-term physiological functional performance *in vivo*.

To further test the durability in bioactivity of heparin bound to the pAMDA coating, the assays of anti-factor Xa and IIa activity by heparin were carried out. Heparin is revealed to bind to antithrombin III (ATIII)

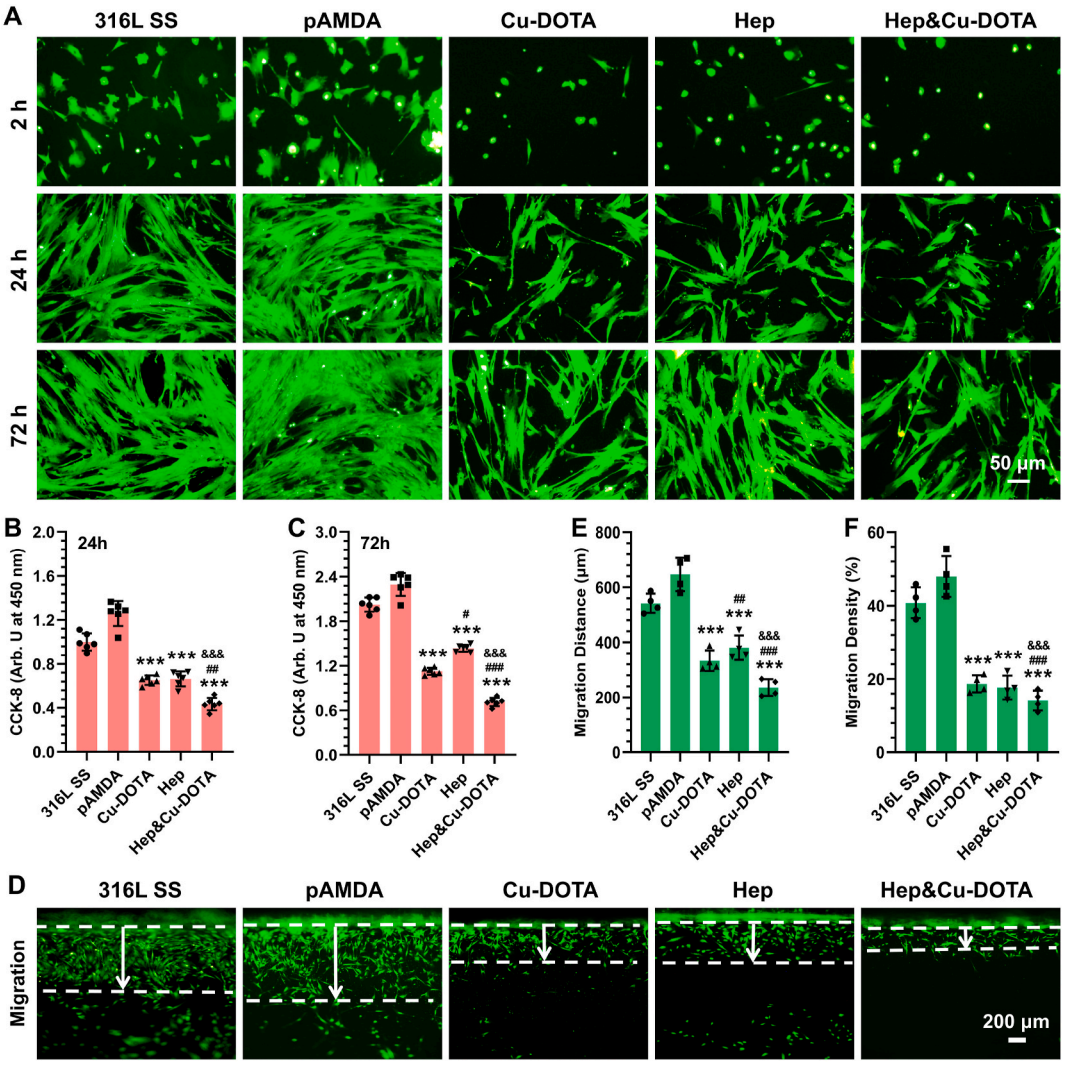

Fig. 4. Adhesion, proliferation and migration of HUASMCs on the non-modified and pAMDA-, Cu-DOTA-, Hep-, and Hep&Cu-DOTA-modified 316L SS. (A) Fluorescence micrographs of HUASMCs grown on the substrates; cell viability after 24 (B) and 72 h (C) of incubation was determined using a CCK-8 kit. (D) fluorescence micrographs of HUASMCs migrated on these surfaces for 24 h. Migration distance (E) and migration density (F) calculated from the fluorescence micrographs. Data are presented as mean ± SD (n = 4) and analyzed using a one-way ANOVA (* compared with pAMDA, # with Cu-DOTA and & with Hep; one symbol indicates $p < 0.05$, two symbols indicate $p < 0.01$ and three symbols indicate $p < 0.005$).

by sulfurized pentosaccharide sequences and then activate it. Thus, the inhibitory effect of activated ATIII on coagulation factors (especially factor Xa and IIa) is increased by thousands of times and prevents thrombus formation [37]. The results revealed that the anti-FXa activity of the Hep and Hep&Cu-DOTA coating was 179 ± 1.3 and 176 ± 1.1 IU/mg, and the anti-FIIa activity was 160 ± 0.8 and 156 ± 0.5 IU/mg, respectively (Fig. 2H and I). Because of the short half-life of heparin, the long-term anticoagulant properties of the Hep&Cu-DOTA coating must be evaluated [38]. Hep&Cu-DOTA samples were immersed in PBS solution for as long as 30 d, and their anti-FXa activity was measured at the same time interval as the NO stability test. After treatment with PBS for 30 d, the anti-Xa activity of the Hep&Cu-DOTA still remained a high value of 98.4 ± 7.1 IU/mg, with ~62.4% of its initial state (Fig. 2J), indicating an excellent retention of heparin activity, and demonstrating that the Hep&Cu-DOTA coating can effectively perform long-term anticoagulant function. Taken together, it was concluded that by using a stepwise synergistic grafting method, a durable endothelium-mimicking coating was successfully created in this work.

3.2. *In vitro cytocompatibility*

For a vascular stent, the ability to support the growth of ECs thus accelerating endothelialization is considered to be a crucial property, because an intact and healthy endothelium is the guarantee of preventing ISR [6]. The major clinical complications that perplex DES are LST and VLST, which have been ascribed to the delayed or incomplete endothelialization by a series of autopsy reports [39]. We found that the modification of 316L SS with pAMDA coating promoted the adhesion (Fig. S5), proliferation (Fig. 3A–C) and migration (Fig. 3D–F) of ECs. This may be attributed to the introduction of positively charged amino groups (Fig. S1 C), which have been widely demonstrated to have excellent cellular affinity based on both the electrostatic attraction and improvement of surface wettability [15]. Considering that the effects of both NO and heparin on EC growth are strongly based on their doses [15,40], in this study, the NO or heparin decorated on the stent surface was strictly controlled at an appropriate concentration (Fig. 2D, F). As expected, the Hep-functionalized surface (Hep) with 800 ng/cm^2 of heparin-grafted density and the NO-functionalized surface (Cu-DOTA) with 5.9 ± 0.3 × 10^{-10} mol cm^{-2} min^{-1} of NO release rate further improved the growth and migration of ECs. The important role of NO in

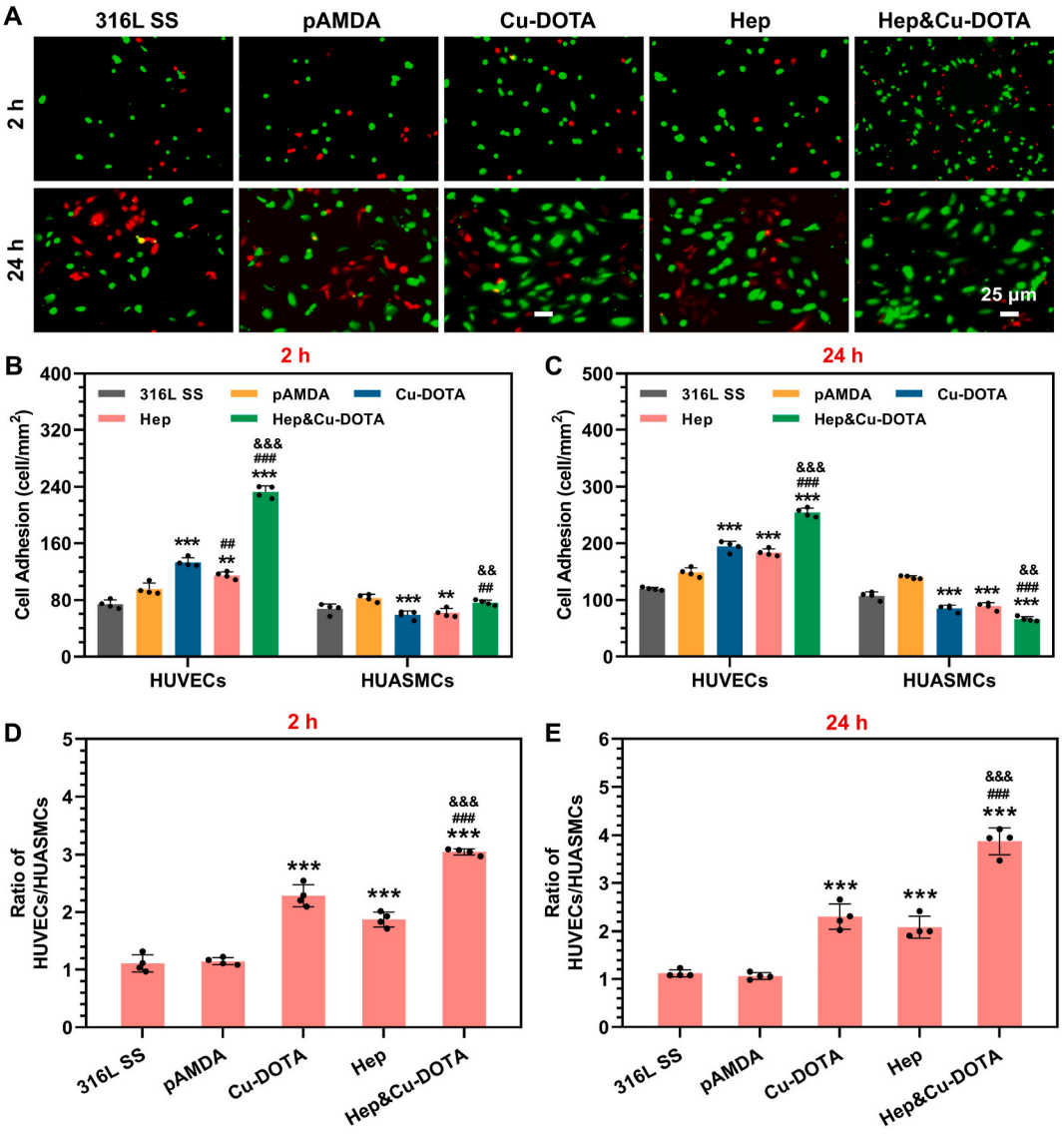

Fig. 5. Competitive growth of HUVECs and HUASMCs on the non-modified and pAMDA-, Cu-DOTA-, Hep-, and Hep&Cu-DOTA-modified 316L SS. (A) Fluorescence micrographs of HUVECs and HUASMCs seeded on these surfaces at equal density and co-cultured for 2 and 24 h, the corresponding quantitative results include the number of adherent cells (B, C), and the ratio of HUVECs to HUASMCs (D, E). Data are presented as mean ± SD (n = 4) and analyzed using a one-way ANOVA (* compared with pAMDA, # with Cu-DOTA and & with Hep; one symbol indicates $p < 0.05$, two symbols indicate $p < 0.01$ and three symbols indicate $p < 0.005$).

regulating EC migration was described in detail in the experiment that VEGF induced angiogenesis [41]. In that experiment, inhibition of NO production blocked the chemotactic actions of VEGF on bovine lung microvascular ECs, while the increase of NO led to an increase of EC migration. As reported, the effect of heparin on the growth and migration of ECs was affected by several factors, including the molecular weight [42] and concentration of heparin, the addition of growth factors and so on [43,44]. In the case of the Hep&Cu-DOTA, it showed substantial promotion in the adhesion, proliferation and migration of ECs, demonstrating the effective synergistic effects via the intergration of NO and heparin in ideal surface decorated doses.

In terms of reducing the complications of stent implantation, surface modification strategies with the only aim of promoting endothelialization usually failed to achieve promising results. For instance, although the Genous™ endothelial progenitor cell (EPC) capturing stent has been reported to be quickly covered with EPCs *in vivo*, it failed to inhibit ISR in clinical trials, which was attributed to the abnormally rapid proliferation of SMC, differentiating from the captured EPCs [45]. In this study, two bioactive molecules were used to functionalize the vascular stents, namely NO and heparin. Both have been reported to inhibit SMC with completely different mechanism. Heparin inhibits SMC by inhibiting cell metabolism [46] and suppressing expression of matrix-degrading enzymes [47], etc; NO inhibits SMC via activating 3′, 5′-cyclic monophosphate (cAMP) signaling pathway [42]. However, some *in vivo* experiments showed that stents modified with single heparin failed to inhibit ISR [8], which may be due to the low amount or/and low activity of the grafted heparin. Actually, one single modification strategy may be insufficient to target the whole complex physiological environment *in vivo*. So another SMC inhibitor, NO, was selected in this study to assist heparin in inhibiting the proliferation of SMC.

The results in Fig. 4 and Fig. S6 showed the adhesion, proliferation and migration of SMCs under the action of single NO, single heparin, and the coordination of both molecules. Fig. S6 showed a significant improvement in SMC adhesion on the pAMDA coating, including increase in cell number and cell area coverage, which may be caused by the large number of amino groups [48]. The covalent grafting of either NO-generating complex or heparin on pAMDA significantly inhibited

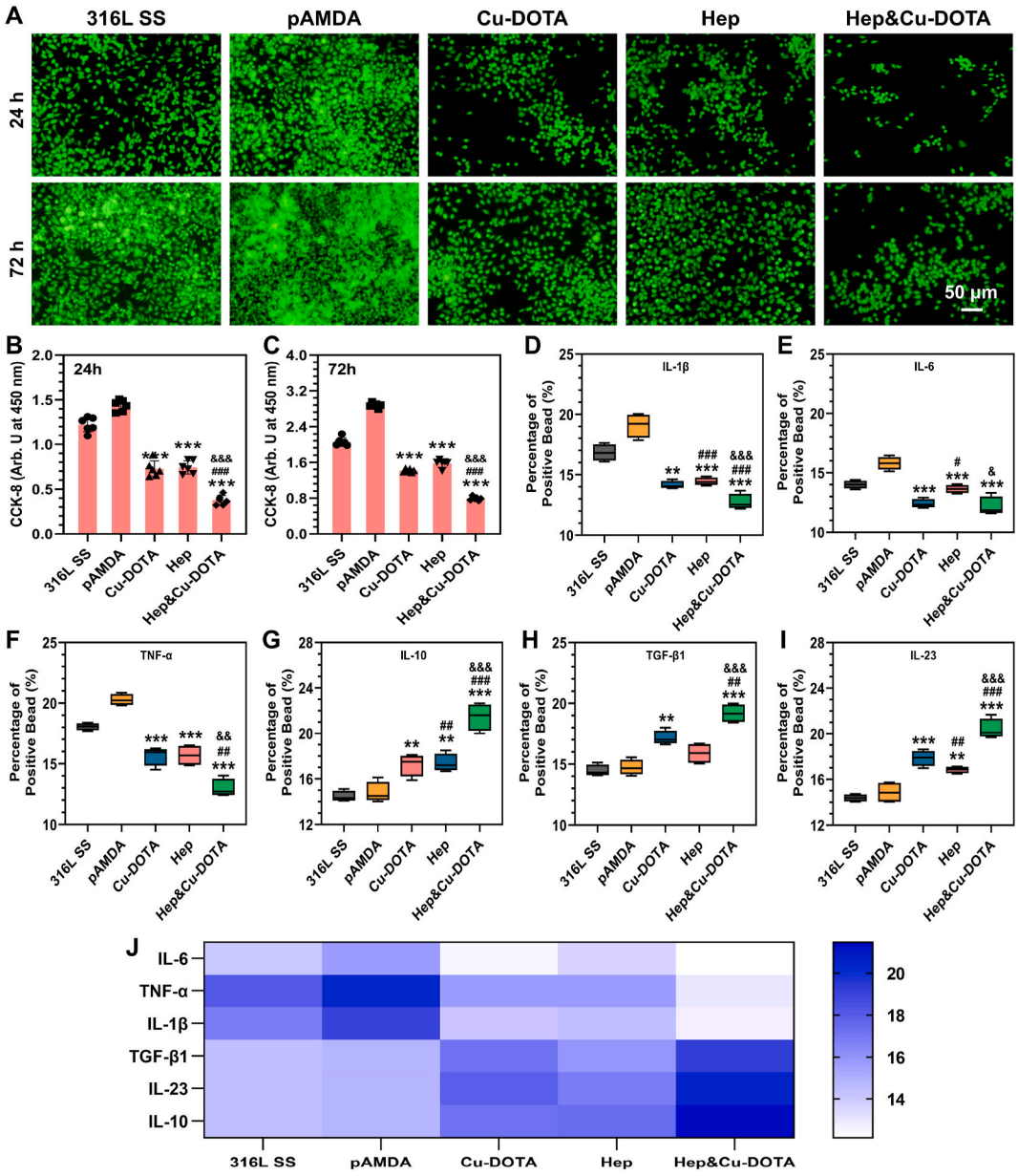

Fig. 6. Adhesion, proliferation, and cytokine expression of macrophages on the non-modified and pAMDA-, Cu-DOTA-, Hep-, and Hep&Cu-DOTA-modified 316L SS. (A) Fluorescence micrographs of macrophaghs on these surfaces. Cell viability after 24 (B) and 72 h (C) of incubation that was determined using a CCK-8 kit. (D-I) The expression of pro-inflammatory (IL-1β, IL-6, TNF-α) and anti-inflammatory (IL-10, TGF-β1, IL-23) cytokines detected by BioLegend Cytometric Bead Array. (J) Heat map of the expression of inflammation-related factors by macrophages grew on these surfaces. Data presented as mean ± SD (n = 4) and analyzed using a one-way ANOVA (* compared with pAMDA, # with Cu-DOTA and & with Hep; one symbol indicates $p < 0.05$, two symbols indicate $p < 0.01$ and three symbols indicate $p < 0.005$).

SMC adhesion in the presence of NO donor, and co-grafting of both molecules resulted in the smallest number and area coverage of the adhered SMCs. Fluorescence images in Fig. 4A and quantitative results of CCK-8 assay in Fig. 4C and D show that both NO and heparin significantly inhibited the proliferation of SMCs, and the inhibitory effect of NO on SMC was stronger than that of heparin. It is worth mentioning that the proliferation of SMCs was significantly lower on the Hep&Cu-DOTA coatings than that on the Cu-DOTA or Hep coating, indicating a synergistic effect between NO and Hep on SMC inhibition. The effect of the aforementioned coatings on the migration of SMCs was consistent with that on the proliferation. The released NO and grafted heparin together induced the strongest inhibition on SMC migration (Fig. 4D), which was reflected in significant decrease in SMC migration distance (Fig. 4E) and migration density (Fig. 4F).

Although NO and heparin have been proved to effectively and synergistically promote EC growth but inhibit SMC growth in a single-cell culture model, it is still necessary to study the growth behavior of both types of cells in a co-culture model, which may be more approximate to the *in vivo* environment for a vascular stent, where the ECs and SMCs interact with each other [49]. In the co-culture experiment, ECs and SMCs were pre-stained with green and red fluorescence, respectively, and seeded on the above coatings at equal density. As was shown in Fig. 5A, both the ECs and SMCs adhered onto the above surfaces can be clearly distinguished via the pre-stained fluorescence, making it feasible to count the cell number. The number of cells adhered in 2 h showed that both NO and heparin significantly improved the adhesion of ECs, and the maximum EC number was achieved under the synergistic action of NO and heparin (Fig. 5B), in consistence with the result of

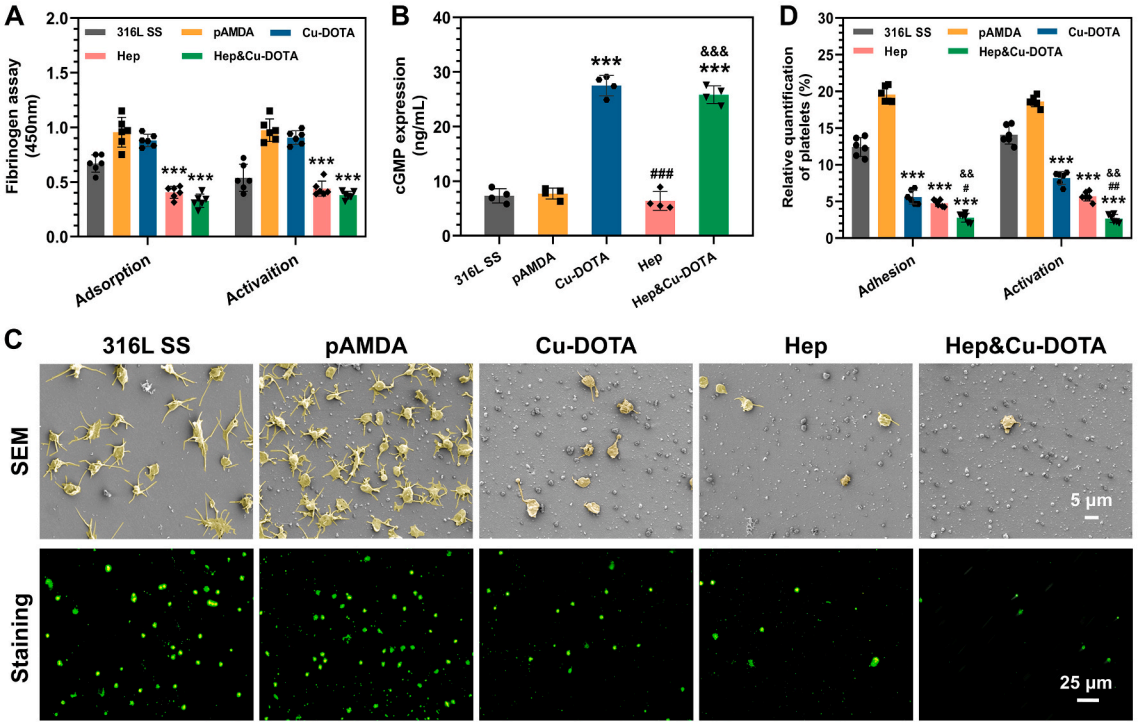

Fig. 7. *In vitro* hemocompatibility of the non-modified and pAMDA-, Cu-DOTA-, Hep-, and Hep&Cu-DOTA-modified 316L SS. (A) Relative amount of the absorbed and activated fibrinogen. (B) cGMP expression of the adherent platelets. (C) SEM and fluorescent images of the adherent platelets and (D) relative quantification of the adherent and activated platelets, in terms of the surface coverage rate of adherent and activated platelets (n = 4). Data are expressed as mean ± SD. * compared with pAMDA, # with Cu-DOTA and & with Hep coating; one symbol indicates $p < 0.05$, two symbols indicate $p < 0.01$, and three symbols indicate $p < 0.005$.

single-cell model in Fig. S5. For SMC adhesion in the co-culture model, either NO or heparin significantly inhibited SMC adhesion (Fig. 5B), thus resulted in obvious adhesion advantage of ECs over SMCs (Fig. 5D). Although the synergistic inhibition between NO and heparin on the initial adhesion of SMCs was not shown in the co-culture model, ECs adhered on the Hep&Cu-DOTA coating still showed the greatest competitive advantage over SMCs, due to the strongest promotion of EC adhesion. The result of competitive adhesion of ECs and SMCs for 24 h was quite similar to that for 2 h, except that the synergistic inhibition of SMCs by NO and heparin was significant in 24 h adhesion on the Hep&Cu-DOTA (Fig. 5E). In total, ECs showed strong competitive advantage over SMCs on the Cu-DOTA, Hep, and Hep&Cu-DOTA coatings after adhesion for 2 and 24 h, and the greatest competitive advantage was obtained on the Hep&Cu-DOTA coating, inferring the superiority of the dual-functional endothelium-mimicking surface in inhibiting intimal hyperplasia, which was usually caused by competitive growth of SMCs over ECs.

The response of inflammatory cells, such as macrophages, to the surface of a deployed stent significantly affects the healing of the stented artery. The incidence of ISR increased gradually with the implantation time in both BMS and DES, which was generally associated with the occurrence of neo-AS [50]. Acute damage to vascular tissue during stent implantation, increased expression of pro-inflammatory factors by ECs induced by blood turbulence behind the stent, and long-term chronic inflammatory response triggered by the stent itself, recruit monocytes. They transform into macrophages, associated with the uptake of oxidized low density lipoprotein, expression of pro-inflammatory factors and necrosis, ultimately leading to the occurrence and progress of neo-AS [51]. Both heparin and NO has been proved to have anti-inflammatory properties [52]. In this study, macrophages were seeded on the above samples, and their proliferation and secretion of pro- and anti-inflammatory factors were determined. The results in Fig. S7 and Fig. 6A, B, and C revealed that amino-rich pAMDA coating promoted the adhesion and proliferation of macrophages compared with the bare 316L SS. In contrast, Cu-DOTA and Hep coating showed significant inhibitory effects on the proliferation of macrophages. Owing to the synergistic effect of NO and heparin, the Hep&Cu-DOTA-functionalized surface resulted in further inhibitory effects on the adhesion and proliferation of macrophages. Moreover, macrophages grown on the Cu-DOTA, Hep and Hep&Cu-DOTA coatings expressed significantly lower amount of pro-inflammatory factors including IL-1β and TNF-α, and higher amount of anti-inflammatory factors including IL-10 and IL-23 than both the bare 316L SS and the pAMDA coating. Among them, the lowest amount of pro-inflammatory factors and the highest amount of anti-inflammatory were realized on the Hep&Cu-DOTA coating.

Although the combined anticoagulant-antiplatelet therapy was continuously optimized in clinic, thrombogenicity is still regarded as one of the major causes of stent failure, including the LST and VLST involved in DES [1]. Tailoring a surface with excellent anti-thrombotic property, therefore, is a frequently applied strategy for vascular stents.

Platelet adhesion and activation, and fibrinogen absorption and conformational change are both the key events during thrombus formation. As shown in Fig. 7A, the deposition of pAMDA coating on the 316L SS induced a significant increase in fibrinogen absorption and activation. In the groups of Cu-DOTA, the production of NO did not resulted in visible changes on both absorption and activation of fibrinogen. In contrast, the grafting of heparin substantially reduced the absorption and activation of fibrinogen. Moreover, we also noted that there was no significant difference in the absorption and activation of fibrinogen between the Hep and Hep&Cu-DOTA groups. Taken together, this may imply there was no directly physiological effect of NO on fibrinogen.

In the case of adhesion and activation of platelets, there was a large number of platelets with protruding pseudopods adhered onto the bare 316L SS. Amine-bearing pAMDA coating aggravated the adhesion and activation of platelets. For the Cu-DOTA coatings, the chelated Cu^{2+} can be reduced into Cu^{+} ions by GSH in the NO donor solution, which then catalyzed GSNO to release NO [33]. NO inhibits platelet aggregation by

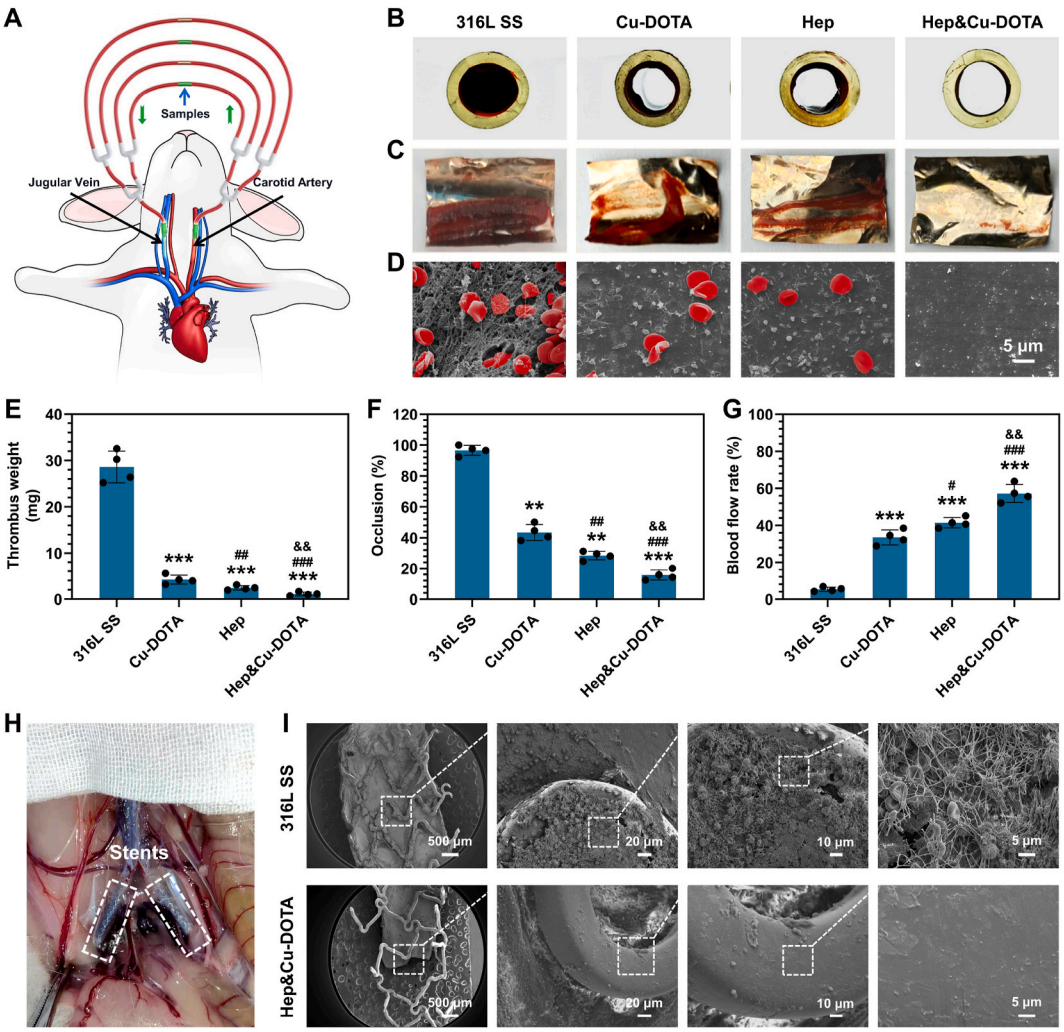

Fig. 8. *Ex vivo* and *in vivo* hemocompatibility evaluation for the bare and modified 316L SS foils (A-G) and vascular stents (H, I). The bare and modified 316L SS foils were installed in arteriovenous shunts of a New Zealand white rabbit (A); optical photographs of the thrombi formed in the PVC tubings installed with the above-mentioned samples (cross-sectional view, B) and those on the flattened samples (C), which were further analyzed by SEM (D); some quantitative results such as thrombus weight (E) on the samples, occlusion rate (F) and blood flow rate (G) of the sample-installed PVC tubings. I*n vivo* hemocompatibility evaluation for the bare and Hep&Cu-DOTA modified 316L SS vascular stents in rabbit iliac arteries (H), the samples were inspected by SEM (I). Data are presented as mean ± SD (n = 4) and analyzed using a one-way ANOVA (*compared with 316L SS, $^{\#}$with Cu-DOTA and $^{\&}$with Hep coating; one symbol indicates $p < 0.05$, two symbols indicate $p < 0.01$, and three symbols indicate $p < 0.005$).

damping the thromboxane A_2 receptor via phosphorylation of cGMP-dependent protein kinase [53]. As expected, the generated NO induced by Cu-DOTA significantly up-regulated the expression of cGMP (Fig. 7B), resulting in significant inhibition in platelet adhesion and activation (Fig. 7C). Similarly, grafting of heparin on the pAMDA coating also resulted in an inhibition of platelet adhesion and activation. Heparin is one of the most essential clinical anticoagulant, which accelerates and amplifies the inhibition of thrombin by antithrombin [8]. Heparin is also widely used for the surface modification of blood contacting materials to reduce platelet adhesion and activation, thus reducing the risk of thrombosis [54,55]. However, heparin treatment can cause thrombocytopenia, which is associated with platelet activation and aggregation [53]. Gao et al. discovered one possible mechanism, that is, heparin bound to integrin αIIbβ3 on the surface of platelets, thus induced phosphorylation of some pivotal cytosolic signaling molecules, such as Akt, and resulted in platelet cell spreading [56]. This challenges the strategy of anticoagulant modification by grafting heparin alone. On the Hep&Cu-DOTA, the released NO and grafted heparin adopt different anticoagulant strategy, thus effectively avoid thrombosis caused by the possible platelet activation by heparin. From the quantification results in Fig. 7D, both numbers of the adhered and activated platelets were significantly lower on the Hep&Cu-DOTA coating than on the Cu-DOTA and Hep coatings, demonstrating that there was a synergistic effect of NO and heparin in the inhibition of platelet adhesion and activation. We also demonstrated that as a newly synthesized material, the pAMDA exhibited a safe hemolysis rate within 1% (Fig. S8).

3.3. *Ex vivo and in vivo anti-thrombogenicity*

To further test the anti-thrombogenicity of the Cu-DOTA-, Hep-, and Hep&Cu-DOTA-functionalized surfaces in blood, *ex vivo* circulation was performed (Fig. 8A). After 2 h of circulation, the PVC tubes with the bare 316L SS foils were almost blocked, but those with Cu-DOTA- or Hep-modified foils were only covered with thin strip of thrombi, and those with Hep&Cu-DOTA coating were almost free of thrombus (Fig. 8 B, C). Analysis by SEM (Fig. 8D) revealed that typical thrombi with platelets and red blood cells (RBCs) wrapped in fibrin networks were formed on the bare 316L SS foils. Thin fibrin networks dotted with some platelets and RBCs were found on the Cu-DOTA- and Hep- modified surfaces. Of

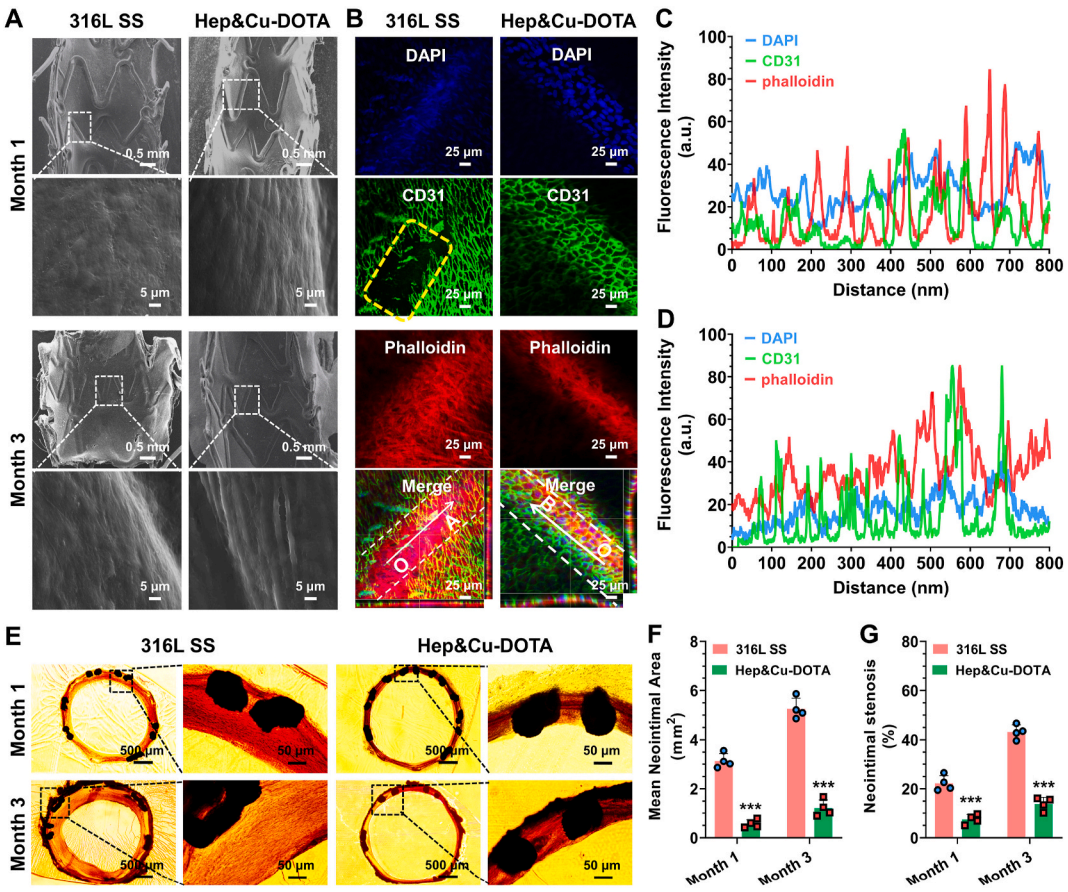

Fig. 9. The bare and modified 316L SS vascular stents with Hep&Cu-DOTA coatings were implanted in rabbit iliac arteries for 1 and 3 months. SEM images of the surfaces of stents implanted for 1 and 3 months indicated the endothelialization degree (A), which was further identified via CD31 immunofluorescence staining of the neointima on vascular stents implanted for 1 month (B) and quantified via fluorescence intensity, (C) for 316L SS and (D) for Hep&Cu-DOTA. Van Gieson staining for hard-tissue-slices of the arteries implanted with vascular stents for 1 and 3 months was carried out to demonstrate the intimal hyperplasia degree (E), then mean neointimal area (F) and neointimal stenosis rate (G) were calculated via Image J. Data are presented as mean ± SD (n = 4) and analyzed using a one-way ANOVA (***$p < 0.001$ compared with 316L SS stent).

special noteworthiness is that there was little tangible substance, such as platelets and RBCs on the Hep&Cu-DOTA-modified foils (Fig. 8 D). The weights of the thrombi were further determined (Fig. 8E). Thrombus weight was significantly decreased on Cu-DOTA or Hep coating, compared with the bare 316L SS, and the least weight was obtained on the Hep&Cu-DOTA foils. Obviously, the thrombus weight on the foil correlated with the occlusion rate (Fig. 8F) and correlated inversely with the blood flow rate of the shunt (Fig. 8G). All the results indicated that the Hep&Cu-DOTA group had the best *ex vivo* antithrombotic properties.

Furthermore, *in vivo* stent implantation was carried out to evaluate the stent blood compatibility, because intimal injury, which has been popularly regarded as one of the most important initiating factors for in-stent coagulation [50] was neglected in the *ex vivo* experiment. Bare and Hep&Cu-DOTA-coated 316L SS stents were symmetrically implanted in both iliac arteries of a rabbit for 2 h (Fig. 8H). SEM results revealed that the bare 316L SS stent was covered with a thick layer of thrombus composed of a mesh of cross-linked fibrin, aggregated platelets and RBCs, whereas there was no detectable thrombosis on the Hep&Cu-DOTA stents. (Fig. 8 I). Taken together, these results indicate that the synergistic action of NO and heparin endows the stent with the almost perfect EC-like thromboresistant properties.

3.4. *In vivo implantation of the Hep&Cu-DOTA-functionalized vascular stents*

To test whether our developed durable Hep&Cu-DOTA endothelium-mimicking coating can effectively address the issues of vascular stents associated with the incomplete endothelialization and intimal hyperplasia, the long-term stent implantation in rabbit was conducted.

After the stents were implanted in the iliac arteries for 1 month, the bare and Hep&Cu-DOTA-modified 316L SS stents were covered with a layer of neotissue. SEM images showed that some of the uncoated 316L SS stent struts were covered with fibrous-like tissues, whereas the Hep&Cu-DOTA-modified stent struts were fully covered with a layer of regularly arranged cells (Fig. 9 A). To identify the type of the cells grown on the vascular stents, immunofluorescence staining for CD31 was performed (Fig. 9 B, Fig. S9 and Vidio S1, S2). Laser confocal microscope analysis revealed that the uncoated stent structs were not completely covered with ECs, consistent with the SEM results. In contrast, a compact endothelial cell layer was formed on the Hep&Cu-DOTA-coated stent structs, which resulted in higher CD31 expression (green line in Fig. 9C) than on the bare stent (green line in Fig. 9D).

Supplementary video related to this article can be found at https://doi.org/10.1016/j.bioactmat.2021.05.009

Cross sections of the arteries implanted with stents for 1 and 3 months, were stained with Van Gieson's to determine the in-stent restenosis. Optical micrographs (OMs) in Fig. 9E showed that the neointima formed on the modified stent was obviously thinner than on the bare one. Quantification of the neointimal area and in-stent stenosis rate were calculated from the OMs by Image J software and analyzed using one-way ANOVA. Hep&Cu-DOTA coating led to significant decreases in both the neointimal area and in-stent stenosis compared to the uncoated

stents (Fig. 9F and G).

Complications of stent implantation, including ISR and LST, are usually ascribed to coagulation, long-term inflammation, migration and proliferation of SMCs, and their excessive extracellular matrix deposition. In the Hep&Cu-DOTA-coating, the covalently grafted heparin enhanced the inactivation of thrombin by ATIII thus inhibited coagulation [8], enhanced growth of ECs while inhibited proliferation of SMCs; the chelated Cu^{2+} ions catalyzed the NO donor in the circulation to continuously generate NO in a range of physiological dose, to promote growth of ECs, and to inhibit coagulation, inflammation, and proliferation of SMCs. Under the synergistic and complementary actions of heparin and NO, the Hep&Cu-DOTA-coated stents led to rapid endothelialization and less in-stent restenosis.

4. Conclusion

In summary, a durable endothelium-mimicking coating has been developed in this study to tailor the required long-term physiological functions of cardiovascular stents. The endothelium-mimicking surface is realized by stepwise covalent grafting of NO-generating species of Cu-DOTA and glycocalyx component of heparin on a durable amine-bearing adhesive pAMDA coating, with high degree of surface chemical cross-linking structure. Our results demonstrated that the combination with durable surface coating and covalent immobilization manner of molecules endowed the endothelium-mimicking surface with about 62.4% of heparin bioactivity retention and up to 81.3% of catalytic activity of NO after application for 1 month. Both the *in vitro* and *in vivo* results indicate that the functionalized vascular stent substantially improved antithrombogenicity, anti-inflammation, anti-restenosis and enhanced re-endothelialization. We envision that such a durable endothelium-mimicking coating could be a promising platform to address the major clinical complications frequently appear at blood-contacting devices.

CRediT authorship contribution statement

Qing Ma: Conceptualization, Methodology, Investigation, Formal analysis, Data curation, Writing – original draft. **Xiuying Shi:** Conceptualization, Methodology, Investigation, Formal analysis, Data curation, Writing – original draft. **Xing Tan:** Methodology, Investigation, Data curation. **Rui Wang:** Methodology, Formal analysis. **Kaiqin Xiong:** Methodology, Investigation, Formal analysis. **Manfred F. Maitz:** Writing – review & editing. **Yuanyuan Cui:** Methodology. **Zhangmei Hu:** Methodology. **Qiufen Tu:** Funding acquisition, Resources, Writing – review & editing. **Nan Huang:** Resources. **Li Shen:** Funding acquisition, Resources. **Zhilu Yang:** Conceptualization, Funding acquisition, Resources, Project administration, Supervision, Writing – review & editing.

Declaration of competing interest

The authors declare that they have no known competing financial interests or personal relationships that could have appeared to influence the work reported in this paper.

Acknowledgments

This work was supported by the National Natural Science Foundation of China (Project 82072072), International Cooperation Project by Science and Technology Department of Sichuan Province (2021YFH0056, 2019YFH0103) and the Fundamental Research Funds for the Central Universities (2682020ZT82, 2682020ZT76). We would like to thank Analytical and Testing Center of Southwest Jiaotong University for SEM and LSCM tests and Shimazu China Co. LTD for XPS test.

Appendix A. Supplementary data

Supplementary data to this article can be found online at https://doi.org/10.1016/j.bioactmat.2021.05.009.

References

[1] T. Palmerini, A.J. Kirtane, P.W. Serruys, P.C. Smits, E. Kedhi, D. Kereiakes, D. Sangiorgi, L. Bacchi Reggiani, C. Kaiser, H.S. Kim, A. De Waha, F. Ribichini, G. W. Stone, Stent thrombosis with everolimus-eluting stents: meta-analysis of comparative randomized controlled trials, Circ. Cardiovasc. Interv. 5 (3) (2012) 357–364.

[2] R. Hoffmann, G.S. Mintz, G.R. Dussaillant, J.J. Popma, A.D. Pichard, L.F. Satler, K. M. Kent, J. Griffin, M.B. Leon, Patterns and mechanisms of in-stent restenosis. A serial intravascular ultrasound study, Circulation 94 (6) (1996) 1247–1254.

[3] H. Kitabata, J.P. Loh, L.K. Pendyala, S. Badr, D. Dvir, I.M. Barbash, S. Minha, R. Torguson, F. Chen, L.F. Satler, W.O. Suddath, K.M. Kent, A.D. Pichard, R. Waksman, Two-year follow-up of outcomes of second-generation everolimus-eluting stents versus first-generation drug-eluting stents for stenosis of saphenous vein grafts used as aortocoronary conduits, Am. J. Cardiol. 112 (1) (2013) 61–67.

[4] K. Goto, Z. Zhao, M. Matsumura, T. Dohi, N. Kobayashi, A.J. Kirtane, L.E. Rabbani, M.B. Collins, M.A. Parikh, S.K. Kodali, M.B. Leon, J.W. Moses, G.S. Mintz, A. Maehara, Mechanisms and patterns of intravascular ultrasound in-stent restenosis among bare metal stents and first- and second-generation drug-eluting stents, Am. J. Cardiol. 116 (9) (2015) 1351–1357.

[5] F. Otsuka, M. Vorpahl, M. Nakano, J. Foerst, J.B. Newell, K. Sakakura, R. Kutys, E. Ladich, A.V. Finn, F.D. Kolodgie, R. Virmani, Pathology of second-generation everolimus-eluting stents versus first-generation sirolimus- and paclitaxel-eluting stents in humans, Circulation 129 (2) (2014) 211–223.

[6] F. Otsuka, A.V. Finn, S.K. Yazdani, M. Nakano, F.D. Kolodgie, R. Virmani, The importance of the endothelium in atherothrombosis and coronary stenting, Nat. Rev. Cardiol. 9 (8) (2012) 439–453.

[7] M. Joner, G. Nakazawa, A.V. Finn, S.C. Quee, L. Coleman, E. Acampado, P. S. Wilson, K. Skorija, Q. Cheng, X. Xu, H.K. Gold, F.D. Kolodgie, R. Virmani, Endothelial cell recovery between comparator polymer-based drug-eluting stents, J. Am. Coll. Cardiol. 52 (5) (2008) 333–342.

[8] Y. Yang, P. Gao, J. Wang, Q. Tu, L. Bai, K. Xiong, H. Qiu, X. Zhao, M.F. Maitz, H. Wang, X. Li, Q. Zhao, Y. Xiao, N. Huang, Z. Yang, Endothelium-mimicking multifunctional coating modified cardiovascular stents via a stepwise metal-catechol-(amine) surface engineering strategy, Research (Washington, D.C.) 2020 (2020), 9203906.

[9] M. Qian, Q. Liu, Y. Wei, Z. Guo, Q. Zhao, In-situ biotransformation of nitric oxide by functionalized surfaces of cardiovascular stents, Bioact. Mater. 6 (5) (2021) 1464–1467.

[10] O. Larm, R. Larsson, P. Olsson, A new non-thrombogenic surface prepared by selective covalent binding of heparin via a modified reducing terminal residue, Biomater. Med. Devices Artif. Organs 11 (2–3) (1983) 161–173.

[11] A.W. Clowes, M.M. Clowes, Kinetics of cellular proliferation after arterial injury. IV. Heparin inhibits rat smooth muscle mitogenesis and migration, Circ. Res. 58 (6) (1986) 839–845.

[12] C.F. Reilly, L.M. Fritze, R.D. Rosenberg, Heparin inhibition of smooth muscle cell proliferation: a cellular site of action, J. Cell. Physiol. 129 (1) (1986) 11–19.

[13] A. Koster, T. Fischer, M. Praus, H. Haberzettl, W.M. Kuebler, R. Hetzer, H. Kuppe, Hemostatic activation and inflammatory response during cardiopulmonary bypass: impact of heparin management, Anesthesiology 97 (4) (2002) 837–841.

[14] L. Stavenow, B. Lindblad, C.B. Xu, Unfractionated heparin and low molecular weight heparin do not inhibit the growth of proliferating human arterial smooth muscle cells in culture, European journal of vascular and endovascular, Eur. J. Vasc. Endovasc. Surg. 10 (2) (1995) 215–219.

[15] Z. Yang, Q. Tu, J. Wang, N. Huang, The role of heparin binding surfaces in the direction of endothelial and smooth muscle cell fate and re-endothelialization, Biomaterials 33 (28) (2012) 6615–6625.

[16] P.A. Hårdhammar, H.M. van Beusekom, H.U. Emanuelsson, S.H. Hofma, P. A. Albertsson, P.D. Verdouw, E. Boersma, P.W. Serruys, W.J. van der Giessen, Reduction in thrombotic events with heparin-coated Palmaz-Schatz stents in normal porcine coronary arteries, Circulation 93 (3) (1996) 423–430.

[17] T. Zubilewicz, J. Wronski, A. Bourriez, P. Terlecki, A.M. Guinault, B. Muscatelli-Groux, J. Michalak, D. Méllière, J.P. Becquemin, E. Allaire, Injury in vascular surgery–the intimal hyperplastic response, Med. Sci. Mon. Int. Med. J. Exp. Clin. Res. 7 (2) (2001) 316–324.

[18] D.J. Suchyta, H. Handa, M.E. Meyerhoff, A nitric oxide-releasing heparin conjugate for delivery of a combined antiplatelet/anticoagulant agent, Mol. Pharm. 11 (2) (2014) 645–650.

[19] Y. Weng, Q. Song, Y. Zhou, L. Zhang, J. Wang, J. Chen, Y. Leng, S. Li, N. Huang, Immobilization of selenocystamine on TiO2 surfaces for in situ catalytic generation of nitric oxide and potential application in intravascular stents, Biomaterials 32 (5) (2011) 1253–1263.

[20] T. Yang, Z. Du, H. Qiu, P. Gao, X. Zhao, H. Wang, Q. Tu, K. Xiong, N. Huang, Z. Yang, From surface to bulk modification: plasma polymerization of amine-bearing coating by synergic strategy of biomolecule grafting and nitric oxide loading, Bioact. Mater. 5 (1) (2020) 17–25.

[21] H. Yu, S. Yu, H. Qiu, P. Gao, Y. Chen, X. Zhao, Q. Tu, M. Zhou, L. Cai, N. Huang, K. Xiong, Z. Yang, Nitric oxide-generating compound and bio-clickable peptide mimic for synergistically tailoring surface anti-thrombogenic and anti-microbial dual-functions, Bioact. Mater. 6 (6) (2021) 1618–1627.

[22] A. Chatterjee, S.M. Black, J.D. Catravas, Endothelial nitric oxide (NO) and its pathophysiologic regulation, Vasc. Pharmacol. 49 (4–6) (2008) 134–140.

[23] M. Kushwaha, J.M. Anderson, C.A. Bosworth, A. Andukuri, W.P. Minor, J. R. Lancaster Jr., P.G. Anderson, B.C. Brott, H.W. Jun, A nitric oxide releasing, self assembled peptide amphiphile matrix that mimics native endothelium for coating implantable cardiovascular devices, Biomaterials 31 (7) (2010) 1502–1508.
[24] Z. Yang, Y. Yang, K. Xiong, J. Wang, H. Lee, N.J.C.o.M. Huang, Metal-phenolic surfaces for generating therapeutic nitric oxide gas, Chem. Mater. 30 (15) (2018) 5220–5226.
[25] H.J. Theunissen, R. Dijkema, P.D. Grootenhuis, J.C. Swinkels, T.L. de Poorter, P. Carati, A. Visser, Dissociation of heparin-dependent thrombin and factor Xa inhibitory activities of antithrombin-III by mutations in the reactive site, J. Biol. Chem. 268 (12) (1993) 9035–9040.
[26] F. Gao, Y. Hu, G. Li, S. Liu, L. Quan, Z. Yang, Y. Wei, C. Pan, Layer-by-layer deposition of bioactive layers on magnesium alloy stent materials to improve corrosion resistance and biocompatibility, Bioact. Mater. 5 (3) (2020) 611–623.
[27] Y. Zhang, Y. Liu, Z. Jiang, J. Wang, Z. Xu, K. Meng, H. Zhao, Poly(glyceryl sebacate)/silk fibroin small-diameter artificial blood vessels with good elasticity and compliance, Smart Mater. Med. 2 (2021) 74–86.
[28] Y. Xiao, W. Wang, X. Tian, X. Tan, T. Yang, P. Gao, K. Xiong, Q. Tu, M. Wang, M. F. Maitz, N. Huang, G. Pan, Z. Yang, A versatile surface bioengineering strategy based on mussel-inspired and bioclickable peptide mimic, Research (Washington, D.C.) 2020 (2020), 7236946.
[29] U. Hedin, G. Daum, A.W. Clowes, Heparin inhibits thrombin-induced mitogen-activated protein kinase signaling in arterial smooth muscle cells, J. Vasc. Surg. 27 (3) (1998) 512–520.
[30] T.L. Cornwell, E. Arnold, N.J. Boerth, T.M. Lincoln, Inhibition of smooth muscle cell growth by nitric oxide and activation of cAMP-dependent protein kinase by cGMP, Am. J. Physiol. 267 (5 Pt 1) (1994) C1405–C1413.
[31] W. Cha, M.E. Meyerhoff, Catalytic generation of nitric oxide from S-nitrosothiols using immobilized organoselenium species, Biomaterials 28 (1) (2007) 19–27.
[32] H. Qiu, P. Qi, J. Liu, Y. Yang, X. Tan, Y. Xiao, M.F. Maitz, N. Huang, Z. Yang, Biomimetic engineering endothelium-like coating on cardiovascular stent through heparin and nitric oxide-generating compound synergistic modification strategy, Biomaterials 207 (2019) 10–22.
[33] N. Lyu, Z. Du, H. Qiu, P. Gao, Q. Yao, K. Xiong, Q. Tu, X. Li, B. Chen, M. Wang, G. Pan, N. Huang, Z. Yang, Mimicking the nitric oxide-releasing and glycocalyx functions of endothelium on vascular stent surfaces, Adv. Sci. 7 (21) (2020), 2002330.
[34] H. Lee, S.M. Dellatore, W.M. Miller, P.B. Messersmith, Mussel-inspired surface chemistry for multifunctional coatings, Science (New York, N.Y.) 318 (5849) (2007) 426–430.
[35] W.D. Zhang, X. Yan, T. Li, Y. Liu, Q.T. Fu, Z.G. Gu, Metal-organic layer derived metal hydroxide nanosheets for highly efficient oxygen evolution, Chem Commun.. (Camb) 55 (38) (2019) 5467–5470.
[36] A.L. Olsson, H.C. van der Mei, H.J. Busscher, P.K. Sharma, Acoustic sensing of the bacterium-substratum interface using QCM-D and the influence of extracellular polymeric substances, J. Colloid Interface Sci. 357 (1) (2011) 135–138.
[37] F.A. Ofosu, G. Modi, A.L. Cerskus, J. Hirsh, M.A. Blajchman, Heparin with low affinity to antithrombin III inhibits the activation of prothrombin in normal plasma, Thromb. Res. 28 (4) (1982) 487–497.
[38] E.A. Nutescu, A. Burnett, J. Fanikos, S. Spinler, A. Wittkowsky, Pharmacology of anticoagulants used in the treatment of venous thromboembolism, J. Thromb. Thrombolysis 41 (1) (2016) 15–31.
[39] D.E. Cutlip, G. Nakazawa, M.W. Krucoff, M. Vorpahl, R. Mehran, A.V. Finn, P. Vranckx, C. Kimmelstiel, C. Berger, J.L. Petersen, T. Palabrica, R. Virmani, Autopsy validation study of the academic research consortium stent thrombosis definition, ACC. Cardiovasc. Interv. 4 (5) (2011) 554–559.
[40] E.M. Stewart, X. Liu, G.M. Clark, R.M. Kapsa, G.G. Wallace, Inhibition of smooth muscle cell adhesion and proliferation on heparin-doped polypyrrole, Acta Biomater. 8 (1) (2012) 194–200.
[41] L. Lamalice, F. Le Boeuf, J. Huot, Endothelial cell migration during angiogenesis, Circ. Res. 100 (6) (2007) 782–794.
[42] A.A. Khorana, A. Sahni, O.D. Altland, C.W. Francis, Heparin inhibition of endothelial cell proliferation and organization is dependent on molecular weight, Arterioscler. Thromb. Vasc. Biol. 23 (11) (2003) 2110–2115.
[43] J.L. Giraux, S. Matou, A. Bros, J. Tapon-Bretaudière, D. Letourneur, A.M. Fischer, Modulation of human endothelial cell proliferation and migration by fucoidan and heparin, Eur. J. Cell Biol. 77 (4) (1998) 352–359.
[44] X. Chen, Y. Gao, Y. Wang, G. Pan, Mussel-inspired peptide mimicking: an emerging strategy for surface bioengineering of medical implants, Smart Mater. Med. 2 (2021) (2020) 26–37.
[45] W.K. den Dekker, J.H. Houtgraaf, Y. Onuma, E. Benit, R.J. de Winter, W. Wijns, M. Grisold, S. Verheye, S. Silber, E. Teiger, S.M. Rowland, E. Ligtenberg, J. Hill, M. Wiemer, P. den Heijer, B.J. Rensing, K.M. Channon, P.W. Serruys, H.J. Duckers, Final results of the HEALING IIB trial to evaluate a bio-engineered CD34 antibody coated stent (Genous™Stent) designed to promote vascular healing by capture of circulating endothelial progenitor cells in CAD patients, Atherosclerosis 219 (1) (2011) 245–252.
[46] Y.P. Au, R.D. Kenagy, M.M. Clowes, A.W. Clowes, Mechanisms of inhibition by heparin of vascular smooth muscle cell proliferation and migration, Haemostasis 23 (Suppl 1) (1993) 177–182.
[47] U. Lindahl, G. Bäckström, M. Höök, L. Thunberg, L.A. Fransson, A. Linker, Structure of the antithrombin-binding site in heparin, Proc. Natl. Acad. Sci. U. S. A. 76 (7) (1979) 3198–3202.
[48] Y. Yang, P. Qi, Y. Ding, M.F. Maitz, Z. Yang, Q. Tu, K. Xiong, Y. Leng, N. Huang, A biocompatible and functional adhesive amine-rich coating based on dopamine polymerization, J. Mater. Chem. 3 (1) (2015) 72–81.
[49] M.D. Lavender, Z. Pang, C.S. Wallace, L.E. Niklason, G.A. Truskey, A system for the direct co-culture of endothelium on smooth muscle cells, Biomaterials 26 (22) (2005) 4642–4653.
[50] H. Jinnouchi, S. Kuramitsu, T. Shinozaki, Y. Tomoi, T. Hiromasa, Y. Kobayashi, T. Domei, Y. Soga, M. Hyodo, S. Shirai, K. Ando, Difference of tissue characteristics between early and late restenosis after second-generation drug-eluting stents implantation - an optical coherence tomography study, Circ. J. 81 (4) (2017) 450–457.
[51] K. Toutouzas, A. Colombo, C. Stefanadis, Inflammation and restenosis after percutaneous coronary interventions, Eur. Heart J. 25 (19) (2004) 1679–1687.
[52] N. Jourde-Chiche, F. Fakhouri, L. Dou, J. Bellien, S. Burtey, M. Frimat, P.A. Jarrot, G. Kaplanski, M. Le Quintrec, V. Pernin, C. Rigothier, M. Sallée, V. Fremeaux-Bacchi, D. Guerrot, L.T. Roumenina, Endothelium structure and function in kidney health and disease, Nat. Rev. Nephrol. 15 (2) (2019) 87–108.
[53] G.R. Wang, Y. Zhu, P.V. Halushka, T.M. Lincoln, M.E. Mendelsohn, Mechanism of platelet inhibition by nitric oxide: in vivo phosphorylation of thromboxane receptor by cyclic GMP-dependent protein kinase, Proc. Natl. Acad. Sci. U.S.A. 95 (9) (1998) 4888–4893.
[54] S. Cassese, R.A. Byrne, T. Tada, S. Pinieck, M. Joner, T. Ibrahim, L.A. King, M. Fusaro, K.L. Laugwitz, A. Kastrati, Incidence and predictors of restenosis after coronary stenting in 10 004 patients with surveillance angiography, Heart 100 (2) (2014) 153–159.
[55] D.J. Maron, J.S. Hochman, H.R. Reynolds, S. Bangalore, S.M. O'Brien, W.E. Boden, B.R. Chaitman, R. Senior, J. López-Sendón, K.P. Alexander, R.D. Lopes, L.J. Shaw, J.S. Berger, J.D. Newman, M.S. Sidhu, S.G. Goodman, W. Ruzyllo, G. Gosselin, A. P. Maggioni, H.D. White, B. Bhargava, J.K. Min, G.B.J. Mancini, D.S. Berman, M. H. Picard, R.Y. Kwong, Z.A. Ali, D.B. Mark, J.A. Spertus, M.N. Krishnan, A. Elghamaz, N. Moorthy, W.A. Hueb, M. Demkow, K. Mavromatis, O. Bockeria, J. Peteiro, T.D. Miller, H. Szwed, R. Doerr, M. Keltai, J.B. Selvanayagam, P.G. Steg, C. Held, S. Kohsaka, S. Mavromichalis, R. Kirby, N.O. Jeffries, F.E. Harrell Jr., F. W. Rockhold, S. Broderick, T.B. Ferguson Jr., D.O. Williams, R.A. Harrington, G. W. Stone, Y. Rosenberg, Initial invasive or conservative strategy for stable coronary disease, N. Engl. J. Med. 382 (15) (2020) 1395–1407.
[56] C. Gao, B. Boylan, J. Fang, D.A. Wilcox, D.K. Newman, P.J. Newman, Heparin promotes platelet responsiveness by potentiating αIIbβ3-mediated outside-in signaling, Blood 117 (18) (2011) 4946–4952.